

## Reviewed Preprint

v1 • October 8, 2024

Not revised

## Reviewed Preprint

v2 • April 7, 2026

Revised by authors

## ✉ For correspondence:

[r.maimon@ucl.ac.uk](mailto:r.maimon@ucl.ac.uk)

**Competing interests:** Scanner time was funded by MeiraGTX via a research sponsorship awarded to UCL. M.M. declares financial interest in MeiraGTX.

**Funding:** See [page 18](#)

**Reviewing editor:** Yanchao Bi, Peking University, China

© 2024, Maimon-Mor et al. This article is distributed under the terms of the [Creative Commons Attribution License](#), which permits unrestricted use and redistribution provided that the original author and source are credited.

# Hierarchical cortical plasticity in congenital sight impairment

Roni O Maimon-Mor<sup>1,2</sup>✉, Mahtab Farahbakhsh<sup>1,2</sup>, Nicholas Hedger<sup>3</sup>, Andrew T Rider<sup>1</sup>, Elaine J Anderson<sup>1,4,5</sup>, Geraint Rees<sup>4,5</sup>, Tomas Knapen<sup>6,7</sup>, Michel Michaelides<sup>1,8</sup>, Tessa M Dekker<sup>1,2</sup>

<sup>1</sup>UCL Institute of Ophthalmology, University College London, London, United Kingdom • <sup>2</sup>Experimental Psychology, University College London, London, United Kingdom • <sup>3</sup>Centre for Integrative Neuroscience and Neurodynamics, School of Psychology and Clinical Language Sciences, University of Reading, Reading, United Kingdom • <sup>4</sup>UCL Institute of Cognitive Neuroscience, University College London, London, United Kingdom • <sup>5</sup>The Wellcome Centre for Human Neuroimaging, University College London, London, United Kingdom • <sup>6</sup>Spinoza Centre for Neuroimaging, Royal Netherlands Academy of Sciences, Amsterdam, Netherlands • <sup>7</sup>Cognitive Psychology, Faculty of Behavioural and Movement Sciences, Vrije Universiteit, Amsterdam, Netherlands • <sup>8</sup>Moorfields Eye Hospital, London, United Kingdom

## eLife Assessment

This **important** study examines the stability and compensatory plasticity in the retinotopic mapping in patients with congenital achromatopsia. It provides **convincing** evidence for a stable mapping of the visual field in V1, alongside changes of the readout from V1 into V3, which shows revised receptive field location and size. This paper would be of interest to scientists studying the visual system, brain plasticity, and development.

<https://doi.org/10.7554/eLife.100404.2.sa3>

## Abstract

A robust learning system balances adaptability to new experiences with stability of its foundational architecture. To investigate how the human brain implements this we used a new approach to study plasticity and stability across hierarchical processing stages in visual cortex. We compare the rod system of individuals born with rod-only photoreceptor inputs (achromatopsia) to the typically developed rod system, allowing us to dissociate impacts of life-long versus transient responses to altered input. Cortical input stages (V1) exhibited high stability, with input-deprived cortex showing no retinotopic remapping and exhibiting structural hallmarks of deprivation. However, plasticity manifested as reorganised read-out of these inputs by higher-order cortex, in a pattern that could compensate for the lower resolution of a rod-only system and its lack of high-density foveal input. We propose that these hierarchical dynamics robustly optimize processing of available input and could reflect a broader principle of brain organisation with important implications for emerging sight-rescue therapies.

## Introduction

Neural systems need to be robust on the one hand but have flexibility to adapt to experience on the other. This places opposing pressures on the formation of the brain's neural architecture. Historically, there have been two central contrasting views: early studies suggested that the brain exhibits remarkable plasticity, with the capacity for significant rewiring and reorganisation in response to new or altered experiences (Baker et al., 2005 [↗](#), 2008 [↗](#); Baseler et al., 2002 [↗](#); Calford et al., 2005 [↗](#); Dilks et al., 2009 [↗](#); Ferreira et al., 2016 [↗](#); Schumacher et al., 2008 [↗](#)). More recent work portrays the brain as a fundamentally stable structure resistant to functional reorganisation even when primary sensory inputs are lost (Adams et al., 2007 [↗](#); Baseler et al., 2011 [↗](#); Goesaert et al., 2014 [↗](#); Molz et al., 2023 [↗](#); Ritter et al., 2019 [↗](#)). Our study reframes this

debate by investigating how adaptations of higher-order processing stages can compensate for stability of sensor-to-cortex connections, offering a new perspective on neuroplasticity through the lens of hierarchical network dynamics.

In the visual domain, the focal point of the debate on plasticity and stability has hinged on the extent to which retinal input deprivation can drive local reorganisation in early visual cortex, for example, for deprived tissue to take on inputs from spared retinal locations (Adams et al., 2007 [↗](#); Baker et al., 2005 [↗](#), 2008 [↗](#); Baseler et al., 2002 [↗](#), 2011 [↗](#); Calford et al., 2005 [↗](#); Dilks et al., 2009 [↗](#); Dumoulin & Knapen, 2018 [↗](#); Ferreira et al., 2016 [↗](#); Goesaert et al., 2014 [↗](#); Haak et al., 2015 [↗](#); Molz et al., 2023 [↗](#); Ritter et al., 2019 [↗](#); Schumacher et al., 2008 [↗](#)). In reality visual impairment is a more global phenomenon, affecting all levels of visual processing, with complex dynamics beyond constricted local retinocortical projection zones (Carvalho et al., 2019 [↗](#)). Investigating these dynamics is crucial for understanding neural plasticity bottlenecks of regenerative treatments under trial in human patients (Fischer et al., 2020 [↗](#); Georgiou et al., 2021 [↗](#); Michaelides et al., 2023 [↗](#)). In these treatments, signal is recovered at the level of the sensory organ, here the eye. If tissue at any downstream processing stage has deteriorated due to inactivation or has adopted new roles, it may be less responsive to its original signals. For groundbreaking sight recovery treatments to reach their full potential, understanding these cascading dynamics in the human brain is now paramount.

We revisit the debate on neuroplasticity and stability by investigating adaptations to altered sensory input across hierarchical cortical processing stages, using the inherited retinal disease achromatopsia as a model. Achromatopsia (also known as rod monochromacy) causes cone photoreceptors in the retina to be inactive from birth (Aboshiha et al., 2014 [↗](#)). This means visual development is purely driven by rod photoreceptors. Rod-mediated vision causes low acuity, a blind spot (scotoma) in the rod-free retina of the fovea, nystagmus (involuntary eye-movements), and no colour vision. In most studies on how the brain adapts to sight loss, a major challenge is accurately matching the sensory input experienced by patients in control individuals with typical sight (Brown et al., 2021 [↗](#); Jones et al., 2020 [↗](#); Macnamara et al., 2021 [↗](#)). This matching is critical for distinguishing neural adaptations to long-term altered visual experience from normal transient responses to varying visual input (Binda et al., 2013 [↗](#); Carvalho et al., 2021 [↗](#); Haak et al., 2012 [↗](#); Hummer et al., 2018 [↗](#)). While normally sighted individuals rely on cone vision most of their waking time, rod only vision can also naturally occur or be induced experimentally (e.g. Barton & Brewer, 2015 [↗](#)). This makes it possible to directly compare lifelong rod-only vision in achromatopsia with transient rod-only experiences in normal sight, distinguishing the long-term neural impacts of altered sensory input from temporary changes within the typical system's range of flexibility.

It remains unclear how the brain adapts to altered retinal input in achromatopsia. Initially, a functional MRI study showed that areas of the early visual cortex, typically receiving only foveal cone input, might reorganise to process input from peripheral rod-containing regions (Baseler et al., 2002 [↗](#)). This suggests potential cortical plasticity. However, recent findings by Molz et al. (2023) [↗](#) present a conflicting view, showing no reorganisation in the deprived primary visual cortex of achromats, and structural signs of deprivation (Molz et al., 2022 [↗](#)). This suggests functional stability. Here, we reasoned that both stability and plasticity in a deprived visual system can co-exist across different cortical processing stages; A high degree of stability in sensor-cortex connections (Haak et al., 2015 [↗](#); Molz et al., 2023 [↗](#)) may be offset by plasticity in downstream regions in the hierarchy, which may exhibit more scope to flexibly adapt and optimise the use of available input.

To test this prediction, we drew on a uniquely large sample of achromats and controls. We first characterised spatial tuning and remapping of V1 in a cone-input deprived visual system to resolve ambiguity of earlier findings. We then used a connective field (CF) modelling approach to assess sampling of V1 information by higher order visual cortex (V3). To truly distinguish long-term adaptations from transient changes to altered input, we took a different approach than prior studies. Rather than only manipulating luminance levels, we utilised the method of silent-substitution (Estévez & Spekreijse, 1982 [↗](#)) to create photoreceptor-specific population receptive

field (pRF) mapping that only stimulates rods. Crucially, this allowed us to obtain well-matched, high-quality rod-driven maps from both achromats and controls, enabling unbiased comparison of rod-mediated responses across the groups.

Using these specialised stimuli to characterise the impacts of purely rod-based vision on the visual systems of achromats and normally sighted controls, we first show that V1 retinotopy presents the hallmarks of a highly robust system. There is no evident remapping of cortical regions that are input-deprived under rod-only viewing circumstances, despite their life-long altered input in achromatopsia. We found that the robustness to long-term altered input in V1, is paired with reorganisation of retinotopic read-out by higher-order visual cortex (V3). A comparison of the visual space organization of V1's connectivity with V3, reveals a shift in the distribution of resources in achromats: more cortical resources in V3 are dedicated to sampling the V1 cortical surface that encodes 1°-4° visual angles - the most foveal areas accessible to rods. Vertices in V3 also sample from fewer V1 vertices, i.e., show a reduction in CF size, effectively increasing its spatial resolution. These changes in the rod-based visual system of achromats could act to compensate for the absence of two features of the cone system that the rod system lacks: its high-density foveal sampling and its overall higher resolution. This may reflect an overarching broader organising principle where hierarchical optimisation processes allow the brain to make more efficient use of the available (in this case atypical) input.

## Results

In three results sections, we characterise the interplay between neural plasticity and stability in achromatopsia across three complementary neural markers: brain structure, spatial tuning characteristics of the functional MRI signal in V1, and the hierarchical retinotopic connectivity patterns that indicate how higher-order visual cortex (V3) samples information from V1.

### Structural analysis

As a proxy of structural integrity, we compared cortical thickness across 8 eccentricity segments of V1 (0°-1°, 1°-2°, 2°-3°, etc.; see [Figure 1B](#)) in a large sample of 31 achromats and 100 controls aged 6-35 years. Data were collated over two scanners. We expected changes in achromats to be largest in the segments representing the central 0°-2° eccentricities of the visual field, encompassing the retinal 'rod-free' zone, an oval of approximately 1.25°x0.96° in size ([Curcio et al., 1990](#)). V1 segments were defined using the Benson atlas ([Benson & Winawer, 2018](#)). The atlas fit procedure uses cortical landmarks on individual brains to predict which viewing eccentricity each cortical vertex is attuned to. This allows us to identify where the representation of these eccentricities would have been given typical development, and investigate what they represent in atypical development.

[Figure 1A](#) shows an increase in cortical thickness in achromats compared to controls only in the foveal projection zone (Controlling for scanner, overall cortical thickness, and age; 0°-1° ANCOVA group effect:  $F_{(1,126)}=9.05$ ,  $p_{unc}=0.003$ ; 1°-2°:  $F_{(1,126)}=7.79$ ,  $p_{unc}=0.006$ ). This increase was not present in more eccentric parts of V1 ( $p_{unc}>0.2$  for all). This pattern is in line with previously reported V1 foveal thickening in adult achromats ([Molz et al., 2022](#)), and moreover suggests that this change is already present in late childhood. A further comparison of the cortical thickness in the foveal projection zones (0°-2°) in V2 and V3 ([Figure 1A](#) right), revealed a trend toward significance in V2 ( $F_{(1,126)}=3.07$ ,  $p=0.08$ ) and a significant effect in V3 ( $F_{(1,126)}=6.32$ ,  $p=0.01$ ). As thicker cortex in early visual areas is a hallmark of visual deprivation from birth ([Jiang et al., 2009](#); [Park et al., 2009](#)), this indicates that the foveal projection zones in achromats may lack retinal input. This provides evidence for stability, because if these cortical areas had substantially reorganised to receive more peripheral retinal input, we would not expect to see this marker of deprivation.

### pRF properties of V1

We next test whether the functional visual-spatial tuning of V1 in a system that has developed using only rod input (i.e., achromats) remains stable or adapts, using population receptive field modelling. Our analyses focus on two types of plasticity. First, we ask what happens to the V1

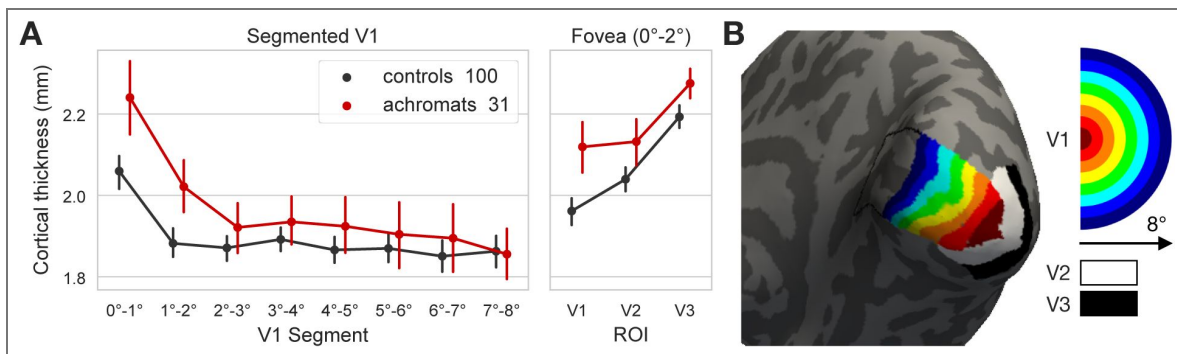


**Figure 1. Structural properties of V1 in achromats and controls.**

(A) Mean V1 cortical thickness of each eccentricity based V1 segment in millimetres (mm). Cortical thickness was increased in achromats (n=31) compared to controls (n=100) only for foveal projection segments 0°-2° and not in more eccentric segments 2°-8°. This pattern was trending in V2 and significant in V3. Error bars are 95% confidence intervals (B) Visualisation of regions of interest in one control participant. Segmentation of V1 to 1° eccentricity bins, and the foveal projection zone (0°-2°) of V2 and V3 was based on the Benson retinotopy atlas (Benson and Winawer, 2018). The half circle on the right shows, in visual space, the area represented by each segment.

cortex normally receiving only cone-mediated input from the foveal ‘rod-free’ zone, which shows structural abnormalities. Second, we test for changes in rod-selective visuospatial tuning across V1 (beyond the 0°-2° ‘rod-free’ fovea), in cortex which normally receives combinations of rod and cone input but develops with only rod inputs in achromats.

V1 receives retinotopically organised input, with adjacent neurons in the cortex receiving signals from adjacent neurons in the retina. Population receptive field modelling links retinotopic voxels in visual cortex to the locations in the visual field they represent (Dumoulin & Wandell, 2008). This is achieved by fitting population receptive fields estimates (pRFs; i.e., Gaussian tuning functions) to BOLD responses evoked by stimuli systematically traversing the visual field. To compare rod-mediated cortex function in achromatopsia to normally developed rod-responses under matched viewing circumstances, we used the silent substitution method (Estévez & Spekreijse, 1982) and low luminance presentation which allowed us to generate stimuli with a rod-isolating contrast (“rod-selective condition”). We also included another stimulus condition that, in a typical retina, stimulates cones and rods equally (“non-selective condition”). This allowed us to assess how rod-mediated measures in both groups compare to more typical pRF measures driven by cones in normally sighted, and whether differences across achromats and controls remain consistent across different visual stimulus properties.

## Coverage and pRF properties of the foveal projection zone

We first compared retinotopic tuning in cortex containing the rod-free foveal projection zone (atlas defined 0°-2°) across controls and achromats. In normally developed retinotopic rod maps, the cortical projection of the foveal rod-free zone, appears as a central “hole” (Figure 2B; Barton & Brewer, 2015). To test if this normally silent area fills in with reorganised retinotopic visual activity in achromats as has previously been reported (Baseler et al., 2002), we compared the percentage of cortex that contains reliable pRFs (coverage; meaning where pRFs could reliably be estimated from visually-driven signal). This is shown in Figure 2 for pRF model fits of  $R^2 > 0.1$ , but effects were similar at  $R^2 > 0.2$  and  $0.3$  (see Supplement 6).

In the rod-selective condition, the coverage in the 0°-2° region of interest was near-identical across achromats and controls (on average 24% in controls, and 25% in achromats,  $t_{(47)} = 0.19$ ,  $p=0.85$ ,  $BF_{10}=0.31$ ; see Figure 2A&B), suggesting no substantial filling in of the foveal projection zone despite life-long rod-only vision. For non-selective stimuli targeting both cones and rods, controls exhibit greater visual coverage (75% on average) compared to achromats, who are missing functional cones (43% on average) (Mann  $U_{(52)}=63$ ,  $p<0.0001$ ; *unequal variance reverted to non-parametric*). Achromats show enhanced coverage under non-selective compared to rod-selective conditions, likely due to increased luminance enhancing the rod system’s signal-to-noise ratio. We note that two achromats show potential filling in, with a foveal activation coverage beyond the 95% predictive interval of the normally sighted rod gap. Their retinotopic profiles (see Supplement 1) suggest this may reflect individual differences in retinal foveal photoreceptor distribution profiles rather than cortical remapping. This highlights the importance of characterising variability in atypically developing populations through larger samples rather than case studies.

Crucially, data quality was matched across groups, with no differences in pRF model fits. Both prior to any  $R^2$  filtering ( $t_{(48)}=0.53$ ,  $p=0.60$ ,  $BF=0.34$ ; see Figure S2b), or after filtering  $R^2 > 0.1$  ( $t_{(48)}=-0.06$ ,  $p=0.95$ ,  $BF=0.31$ ). It is therefore unlikely that any coverage inside the rod “hole” in achromats was masked by low data-quality differences between the groups. In addition, it is unlikely that these findings can be explained by pRF fitting-related artefacts (Binda et al. 2013), as modelling the rod-scotoma in the pRF fitting procedure led to similar results (see methods and Supplement 3).

Another potential confound in our findings is fixation instability. In pRF mapping, which is usually conducted under photopic (cone-dominant) conditions, unstable fixation can cause a signal drop in the foveal projection zone. As expected due to nystagmus, the achromatopsia group showed higher fixation instability compared to controls (*rod-selective*:  $t_{(9,08)}=-3.19$ ,  $p=0.01$ ; *non-selective*:  $t_{(9,41)}=-4.88$ ,  $p<0.001$ ; *degrees-of-freedom corrected for unequal-variance*; see Supplement Figure S2a). However, several lines of evidence suggest this instability cannot fully account for the lack

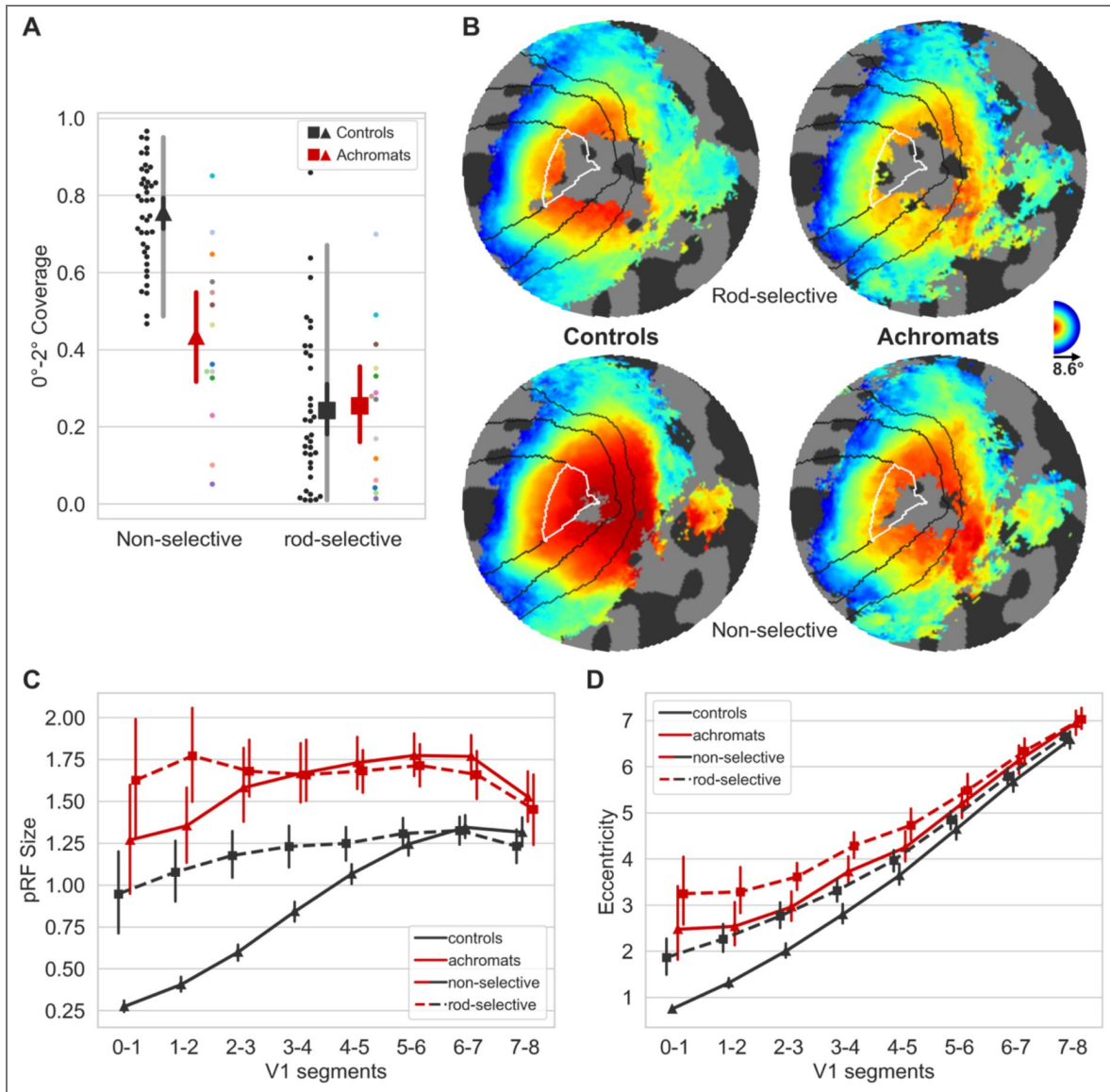


**Figure 2. pRF properties of V1 in achromats and controls.**

(A) Foveal projection zone (0°-2°) coverage. Coverage is the fraction of vertices within the foveal confluence that contain visual information (i.e., pRF  $R^2 > 0.1$ ). Achromats (red markers) are not significantly different from controls (black markers) in the rods only condition (square markers), and do not show complete filling in even in the non-selective condition with higher contrast (triangle markers). Triangle markers: group mean for the non-selective condition, square markers: group mean for the rods only condition. Black markers: controls group mean, red markers: achromat group means. Black/red vertical lines around the mean: 95% confidence interval, grey shaded lines: 2.5%-97.5% percentile interval (only in controls). For achromats, participants' dots are colour-coded to match across conditions and measures (B) Group eccentricity plots on a flat surface for each condition (in standard fsaverage space), presenting the group median value of each vertex. For visualisation purposes, vertices that were absent in more than 30% of the group were left blank in each condition. Black lines denote atlas-based delineations of V1,2,3; white lines mark the foveal projection zone (0°-2°) in V1. As shown in (A) we see no evidence of 'filling in' of the rod scotoma in achromats. (C) pRF sizes along the atlas V1 segments. Achromats show a consistent increase in pRF size compared to controls. (D) Eccentricity of modelled pRFs along the atlas V1 segments. Achromats show an increase in eccentricity compared to controls, however that shift is not consistent across the two stimuli types. Vertical lines in C&D represent 95% confidence intervals.

of "filling in" in achromats. First, within the achromat group, we found no correlation between fixation stability and coverage (*rod-selective: spearman- $r_{(8)}$  = -0.36, p=0.31; non-selective spearman- $r_{(8)}$  = 0.07, p=0.85*); Individuals with more stable, control-like fixation did not show more signal inside the scotoma (see Supplement 2 [↗](#)). Second, in adults with achromatopsia, typically with less severe nystagmus (Kohl et al., 1993 [↗](#)), two recent studies also found absence of filling in (Anderson et al., 2024 [↗](#); Molz et al., 2023 [↗](#)).

So, while we cannot fully exclude nystagmus masking foveal signals in the cortex of some patients, this converging evidence from structural and functional MRI measures across different studies and groups, strongly suggests that the deprived cortex does not substantially 'fill in' with peripheral rod inputs in achromatopsia.

Together these results provide strong evidence for stability in the face of life-long deprivation, i.e., the conservation of the sensory topography.

## Altered rod representation in V1 - pRF size and eccentricity

We next tested for differences in spatial tuning across V1 regions that typically receive both rod and cone inputs but develop with only rod inputs in achromatopsia. Figure 2C [↗](#) shows that pRF sizes in achromats are systematically larger compared to controls across all eccentricities. This holds true for both the non-selective (V1 segments: 2°-3°:  $t_{(52)}=12.57, p_{unc}<0.001$ ; 3°-4°:  $t_{(52)}=11.12, p_{unc}<0.001$ ; 4°-5°:  $t_{(52)}=9.54, p_{unc}<0.001$ ; 5°-6°:  $t_{(52)}=7.52, p_{unc}<0.001$ ; 6°-7°:  $t_{(52)}=5.76, p_{unc}<0.001$ ; 7°-8°:  $t_{(52)}=2.36, p_{unc}=0.022$ ; all segments remain significant after FDR correction), and rod-selective stimulus conditions (V1 segments: 2°-3°:  $t_{(48)}=3.83, p_{unc}<0.001$ ; 3°-4°:  $t_{(48)}=3.67, p_{unc}<0.001$ ; 4°-5°:  $t_{(48)}=4.68, p_{unc}<0.001$ ; 5°-6°:  $t_{(48)}=4.74, p_{unc}<0.001$ ; 6°-7°:  $t_{(48)}=3.98, p_{unc}<0.001$ ; 7°-8°:  $t_{(48)}=2.00, p_{unc}=0.051$ ; all segments but the 7°-8° remain significant after FDR correction). In the non-selective condition, the smaller pRFs in controls are in line with the higher spatial resolution of the cone system, which is not active in the achromat group. However, for the rod-selective condition where both groups activate the same class of photoreceptors, the enlarged pRFs in achromats might indicate altered rod-based visual processing.

Larger pRFs indicate that neuronal populations in achromats' V1 cortex, combine information across larger areas in visual space than in typically sighted controls. This could reflect true neural tuning differences as well as be driven by larger eye movement. However, fixation instability in achromats does not significantly correlate with pRF size in our sample (*rod-selective: spearman- $r_{(8)}$  = -0.41, p=0.24; non-selective spearman- $r_{(8)}$  = -0.37, p=0.29*).

Figure 2D [↗](#) shows that pRF estimates in achromats have higher eccentricities across V1 compared to controls, spanning all tested V1 segments (group comparisons of the rod-selective conditions: 2°-3°:  $t_{(48)}=3.32, p_{unc}=0.002$ ; 3°-4°:  $t_{(48)}=4.42, p_{unc}<0.001$ ; 4°-5°:  $t_{(48)}=3.59, p_{unc}=0.001$ ; 5°-6°:  $t_{(48)}=3.17, p_{unc}=0.003$ ; 6°-7°:  $t_{(48)}=3.15, p_{unc}=0.003$ ; 7°-8°:  $t_{(48)}=2.23, p_{unc}=0.030$ ; all segments but the 7°-8° remain significant after FDR correction). This slight outward eccentricity shift could reflect true changes in neural tuning. However, in the non-selective condition in achromats, even though still only rods are being stimulated, estimated eccentricities are lower than those observed under the rod-selective condition. In fact, the eccentricity estimates of the non-selective condition in achromats appear similar to those of the rod-selective condition in controls. This raises the possibility that pRF position fitting is sensitive to signal-to-noise differences across stimuli, and shows that it is possible, in the achromat system, to obtain eccentricity estimates in the normal rod range.

It has been shown that fitting artefacts around scotoma edges, can give rise to similar outward eccentricity shifts (Binda et al., 2013 [↗](#)). However, when accounting for fitting artefacts around the foveal scotoma edge by modelling the rod-free zone during pRF fitting, pRF size and eccentricity differences remain unchanged (see Supplement 3). Finally, we found no significant correlations between gaze stability and the eccentricity shift (*rod-selective: spearman- $r_{(8)}$  = 0.58, p=0.08; non-selective spearman- $r_{(8)}$  = 0.09, p=0.8, see Supplement 4D*)

Together, these analyses reveal subtle differences in how V1 of achromats responds to rod signals outside the foveal zone, which are consistent with results from other studies (Molz et al. 2023 [↗](#), Anderson et al. 2024 [↗](#)). While we found no direct evidence that these are being driven by confounding factors such as eye-movements or fitting artefacts, more work is needed to understand the underlying processes that give rise to these shifts.

## Connective field modelling – hierarchical sampling

We next used connective field modelling to test whether V3's sampling along the V1 cortical surface in achromatopsia remains stable given the evidence that the foveal part of V1 remains visually silent from birth. We test for two hypothetical types of hierarchical plasticity: shifts in where along the V1 surface V3 samples its information from (CF centre), and shifts in the extent of the area along the V1 surface that V3 samples from (CF size).

Higher-order visual regions receive retinotopic information from V1, with individual neurons sampling information across multiple neighbouring V1 neurons. Connective field (CF) modelling is a functional connectivity-based extension of pRF modelling which characterises this sampling process, based on time-series correlations. While pRF modelling is 'stimulus referred', estimating a voxel's spatial tuning properties based on its response to stimulus variations, connective field modelling is 'neural-referred', estimating a voxel's 'connective field' based on its correlations with aggregated voxels along the V1 surface. Responses throughout cortex are modelled as deriving from Gaussian shaped sampling profiles over the V1 cortical surface (connective fields), defined by a position (centre of the Gaussian) and size (Gaussian spread in mm ( $\sigma$ )) (see illustration in Figure 4C [↗](#)). CF modelling can thus reveal the topographic profile of a brain region's neural connectivity with V1, including the spatial location and extent of sampling. After estimating connective fields, the CF positions can be combined with the retinotopic map of V1 to 'project' the retinotopy of V1 onto the rest of the brain, thereby performing connectivity-derived retinotopic mapping. To create V3 connective-field-based eccentricity maps (Figure 3B [↗](#)), each vertex was assigned the eccentricity of the V1 segment of its connective field centre. Because CF modelling relies on inherent signal fluctuations and involves no assumptions about visual input, it is more robust to potential confounds such as poor fixation and low visual responsiveness (Tangtharakul et al., 2023 [↗](#)). Here we focus on connective fields between V3 and V1. We omit V2, which shares a border with V1, to avoid inaccuracies in CF estimation due to mis-delineation.

## Shifts in V3 resource distribution along the V1 eccentricity map

When both rods and cones are stimulated in the normally sighted system, the largest proportion of V3 voxels is dedicated to sampling information from the V1 foveal projection (connective field centres in the 0°-1° degree range), with a gradual decrease in resources allocated to larger eccentricities (Figure 3A [↗](#)). When only rods are stimulated, foveal sampling is attenuated but the overall pattern of a gradual decrease in sampling from small to larger eccentricities remains. In achromats, the way in which V3 samples V1 is drastically different, with most V3 resources dedicated to sampling eccentricities at 1°-4° for both stimulation conditions (Figure 3B [↗](#)). When comparing the rod-selective condition in achromats to that of controls, we observe a shift towards greater V3 sampling from the V1 cortex encoding the (1°-4°) paracentral visual field (0°-1°:  $t_{(47)}=1.18$ ,  $p_{unc}=0.242$ ; 1°-2°:  $t_{(47)}=4.03$ ,  $p_{unc}<0.001$ ; 2°-3°:  $t_{(47)}=5.32$ ,  $p_{unc}<0.001$ ; 3°-4°:  $t_{(47)}=3.70$ ,  $p_{unc}=0.001$ ; 4°-5°:  $t_{(47)}=2.32$ ,  $p_{unc}=0.025$ ; 5°-6°:  $t_{(47)}=0.84$ ,  $p_{unc}=0.405$ ; 6°-7°:  $t_{(47)}=-0.97$ ,  $p_{unc}=0.337$ ; 7°-8°:  $t_{(47)}=1.93$ ,  $p_{unc}=0.060$ ; segments including 1°-4° remain significant after FDR correction). It is unlikely that these differences result from differences in measurement quality, because the goodness of fit (CF  $R^2$ ) was comparable across the two groups (Supplement 4). We therefore hypothesise that this shift in sampling reflects increased neural resources dedicated to the most fovea-adjacent information that is available to the rod-only system. Surprisingly, even though we found no evidence of visually-driven signal in the region on V1's surface that normally takes foveal input (0°-1°) in achromats (see Figure 2 [↗](#)), there is still a substantial portion of V3 vertices (15%) that sample from this region. This remaining foveal connectivity between V1 and V3 shows that there is also a degree of stability across retinotopic hierarchical sampling.

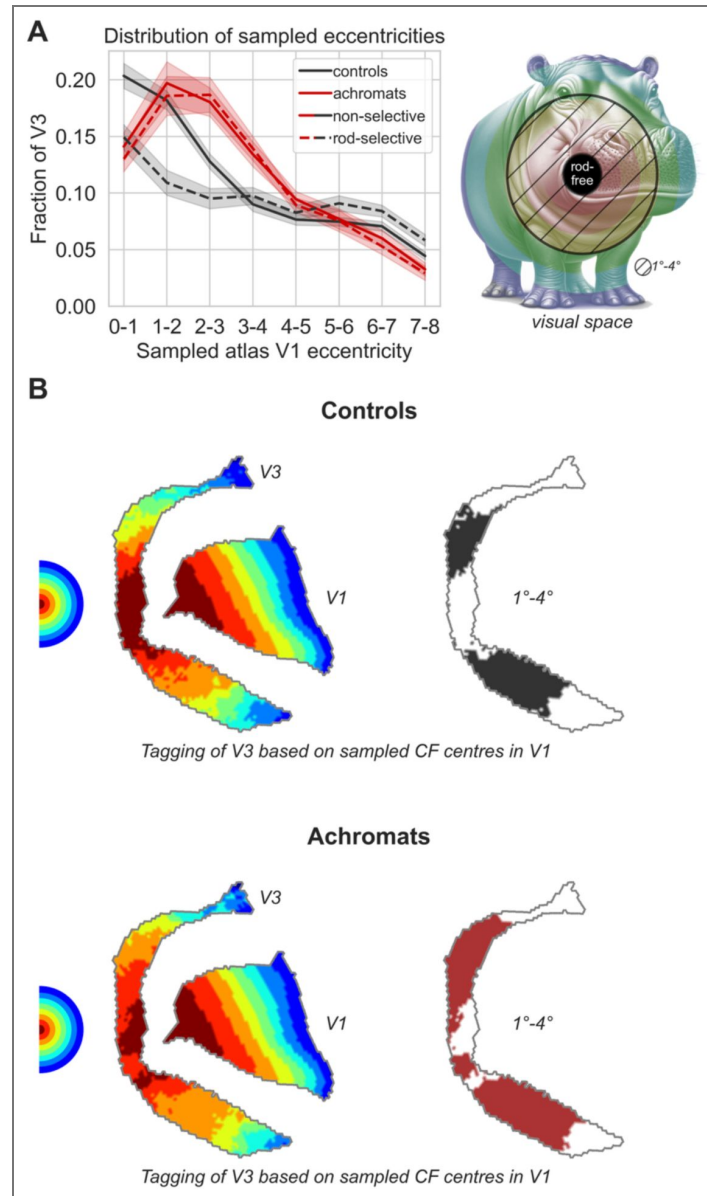


**Figure 3. Connective field modelling (V3) in achromats and controls – sampled eccentricities.**

(A) Left: The fraction of all vertices within V3 that sample from V1, binned by sampled V1 atlas eccentricity. In achromats there is a shift towards greater sampling from the most foveal area that contains rods (1°-4°) of V1 relative to the normally sighted rod and cone systems. Shaded areas: standard errors of the mean (s.e.m). All V1 eccentricities are derived from the Benson Atlas. Right: A schematic illustration of the sampled eccentricities in visual space. Dashed area represents the area where group differences in sampling were found, 1°-4°.

(B) Visualisation of V3 sampled eccentricities of V1 in the rod-selective condition. From left to right: Half circle represents the visual field, where each colour represents 1 visual degree. V1 is colour-coded into segments based on the atlas-assigned eccentricities. Each vertex in V3 is then coloured based on the centre of Gaussian connective field within the V1 surface. Values in V3 are based on group medians. To further highlight the group differences in the amount of cortical surface devoted to the 1°-4° V1 segments we visualise V3 again on the right, colouring in all vertices with a CF centre at the 1°-4° segments.

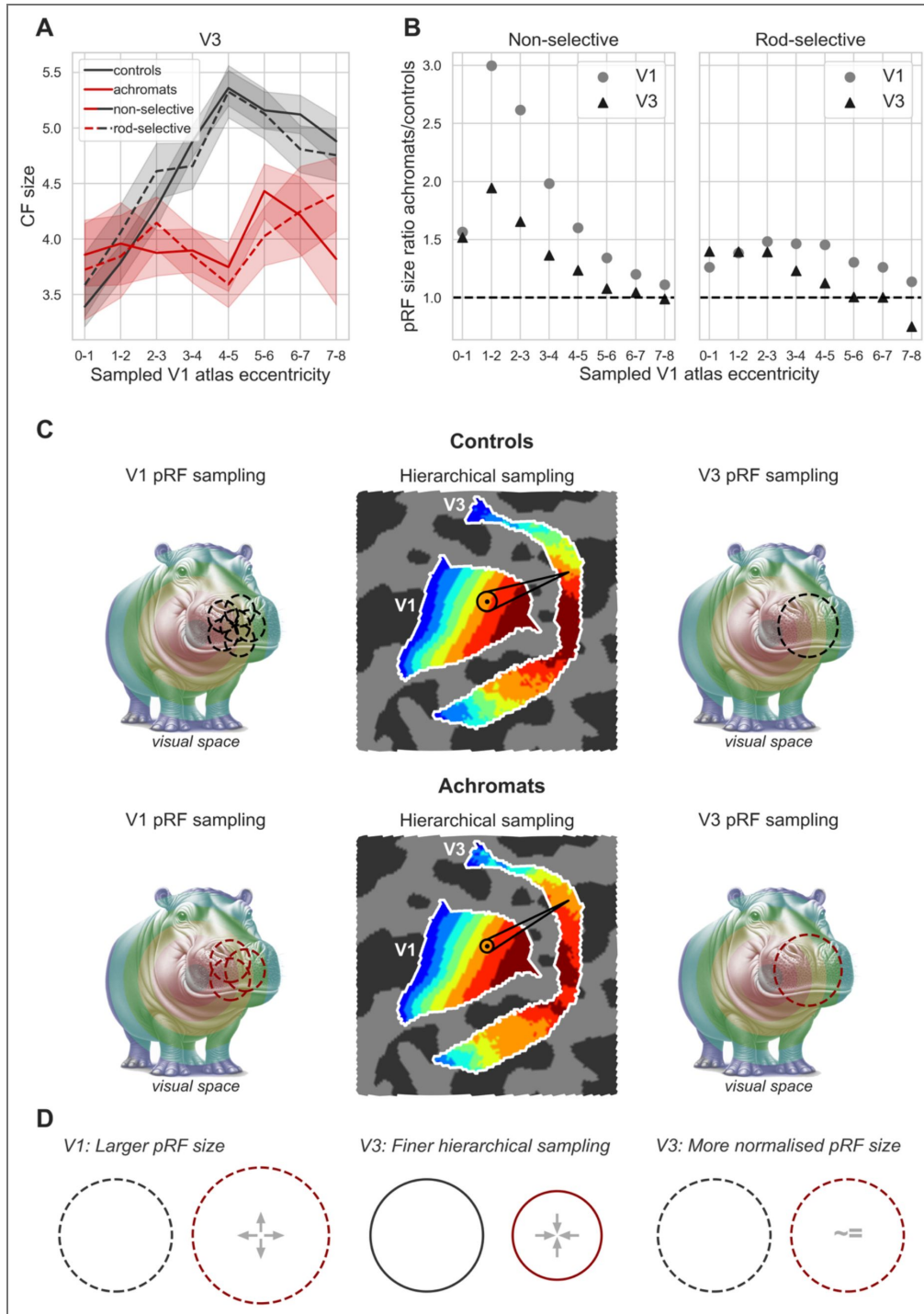


**Figure 4. Connective field modelling (V3) in achromats and controls – connective field size and relationships with pRF size.**

(A) CF sizes in V3 in achromats and controls across the rod-selective and non-selective condition. Controls show an expected increase in CF size with sampled eccentricity while achromats show a flat pattern, with smaller CFs between 4°-6°. In both groups results are consistent across the two stimulation conditions. (B) Ratio of pRF size between achromats and controls in V1 (circles) and V3 (triangles). A ratio of 1 indicates the mean pRF size of achromats is equivalent to that of controls. Across both non-selective (left) and rod-selective (right) stimulus conditions, the ratio of pRF sizes in V3 is closer to 1 than in V1, pointing towards a possible normalising effect of CF size on pRF size. (C) Illustrations depicting the differences in pRF and CF sizes across the groups. (D) A summary of the proposed model of how smaller CF sizes in V3 of achromats might operate as a compensatory mechanism for increased pRF size in V1, resulting in normalized pRF size at the level of V3.

## Shifts in the V3 read-out aperture (CF size) from V1

Figure 4 shows that in normally sighted individuals, connective field size in V3 increases with eccentricity, whether stimulating both rods and cones at the same time, or only rods. This replicates findings by Haak et al., (2013) and Knapen (2021). In achromatopsia, however, V3 connective field sizes remain consistently small across all eccentricities, and are significantly smaller than in the normally sighted rod-system between 4°-6° eccentricity (comparing achromats vs control rod-selective condition: 0°-1°:  $t_{(44)}=1.07$ ,  $p_{unc}=0.289$ ; 1°-2°:  $t_{(45)}=-0.41$ ,  $p_{unc}=0.684$ ; 2°-3°:  $t_{(45)}=-0.58$ ,  $p_{unc}=0.568$ ; 3°-4°:  $t_{(46)}=-1.70$ ,  $p_{unc}=0.097$ ; 4°-5°:  $t_{(47)}=-3.55$ ,  $p_{unc}=0.001$ ; 5°-6°:  $t_{(47)}=-2.63$ ,  $p_{unc}=0.011$ ; 6°-7°:  $t_{(47)}=-0.81$ ,  $p_{unc}=0.420$ ; 7°-8°:  $t_{(45)}=-0.73$ ,  $p_{unc}=0.469$ ; degrees of freedom vary as not all participants have vertices sampling all V1 segments). These smaller connective field sizes in V3, mean that V3 vertices pool across a smaller number of vertices along the V1 cortical surface (4C, middle). The significant CF size differences are unlikely to be a model-fitting bias around a scotoma edge, as V3 vertices sampling from the immediate vicinity of the scotoma (1°-3°) show CF sizes comparable to controls. The significant reduction in CF size occurs only further in the periphery (4°-6°), in regions that are primarily stimulus-driven.

To understand how this finer cortical sampling in V3 (smaller connective fields) impacts visual processing, we consider its effect on population receptive fields (pRFs). In V1, pRF sizes in achromats were significantly larger than in controls for both stimulus conditions, indicating coarser spatial tuning at the cortical input stage (Figure 4C, left). By selectively sampling from a smaller area of the V1 surface (smaller CFs), V3 can effectively compensate for this coarser input. If so, this process should result in a relative normalisation of pRF size in V3 compared to V1 (Figure 4C, right).

To test this prediction, we plotted the ratio of pRF sizes between achromats and controls, where a value of 1 indicates parity between the groups (Figure 4B). As our compensatory connective field hypothesis predicts, the ratio was closer to 1 in V3 than in V1 across both stimulus conditions, confirming the pRF size difference was significantly reduced at the higher cortical stage. Together this shows converging evidence across the two models (pRF and CF) of hierarchical refinement as a possible compensatory mechanism, where V3's altered connectivity helps to normalize the processing of degraded sensory input from V1.

## Discussion

To test the effects of long-term altered visual input on neural plasticity across the cortical hierarchy, we compared a unique group of individuals who have developed only with rod photoreceptor inputs (achromatopsia) to normally sighted individuals who spend most of their waking time relying on cone-dominated vision. As normally sighted can also experience rod-only vision under specific circumstances, this allowed us to dissociate the effects of life-long altered experience from transient altered sensory input. By integrating markers of plasticity and stability across structural, representational, and connectivity analyses we reveal system-level dynamics of stability and adaptations to altered visual experience. The results offer a new perspective on neural plasticity and stability, recasting these processes as two interacting forces acting simultaneously on the cortex rather than two separate neural responses to change.

Specifically, in achromatopsia we found thickening of the cortex around the foveal projection zone, which receives only cone-photoreceptor inputs and therefore would be signal-deprived from birth in this group. In contrast to early reports (Baseler et al., 2002), we found no evidence that visually-induced signalling inside this region had increased compared to the typically developed rod system. We also observed subtle functional changes in V1 retinotopic tuning including increased population receptive field sizes, however their origins are unclear. These data reveal that visual spatial representations in V1 are largely stable in the face of chronic, highly atypical retinal input, integrating and resolving ambiguity of earlier findings (Baseler et al., 2002; Mckyton et al., 2021; Molz et al., 2022, 2023). This high stability at the cortical input-stage contrasted with reorganisation of the read-out of these inputs by higher-order visual cortex. Notably, more cortical resources in V3 were dedicated to sampling input from the near-fovea, and

V3 neuron populations aggregated information across smaller areas along the V1 cortical surface. There was also evidence for stability of sampling in achromatopsia, because V3 retained connectivity with the foveal confluence despite the life-long scotoma.

Together these findings show that while primary sensory areas such as V1 exhibit considerable stability, higher-order areas such as V3 display marked plasticity that may optimise use of the available information. Both increased sampling of the most fovea-adjacent information available to rods, and finer-grained sampling of coarser inputs could effectively counteract the limitations of developing with a fully rod-based system. These findings add a new dimension to the ongoing debate on neural plasticity versus stability by proposing a hierarchical network perspective where both processes interact across processing stages to maintain the integrity of foundational architecture, whilst optimizing the processing of available input.

Several control measures and analyses presented above show that it is unlikely that these results are artefacts of data quality or eye movements. Model fits were comparable across achromat and control groups, ruling out data quality discrepancies as an explanation for the observed differences. Furthermore, converging evidence shows that the lack of 'filling in' in the V1 cortex of achromats is unlikely to be obscured by nystagmus (Supplement 2). First, eye-tracking data in achromats showed no correlation between fixation stability and foveal cortex activity. Second, our finding is consistent with two recent studies on adults with achromatopsia who show less severe nystagmus (Kohl et al., 1993 [↗](#)), which also found no evidence for filling in (Anderson et al., 2024 [↗](#); Molz et al., 2023 [↗](#)). Most crucially, a lack of filling in is aligned with the structural and connectivity analyses revealing corroborating markers of cortical deprivation in line with the pRF mapping result: the deprived V1 foveal projection zone was thickened, and V3's cortical sampling was shifted away from it.

The hierarchical reorganisation observed in V3 is unlikely to be driven by fixation instability. Connective field (CF) estimates are robust to eye movements (Tangtartharakul et al., 2023 [↗](#)), because they are anchored to V1 inputs rather than absolute screen position. Considered alone, the pRF results could alternatively be explained by eye movements introducing a fixed size offset that affects smaller V1 pRFs more strongly than those in V3. While we found no evidence for this relationship between pRF size and gaze measures in our patients, we cannot fully rule out the possibility. Nevertheless, the internal consistency between the CF and pRF measures provides a more parsimonious account; that sampling across the hierarchy accounts for coarser tuning at the input stage.

There are convincing arguments for the importance of a system that maintains highly stable sensor-to-cortex connections at the first cortical input stage. Re-routing of cortical projections in response to changing visual signals could lead to "coding catastrophe", because left unchecked it could leave visual processing areas throughout the brain with mislabelled retinotopic signals, corresponding to different regions of visual space than they would normally represent (Dumoulin & Knapen, 2018 [↗](#); Haak et al., 2015 [↗](#); Wandell & Smirnakis, 2010 [↗](#)). Higher-order regions aggregate more inputs across visual space and other sensory domains, and display greater invariance to low-level stimulus properties (Lehky & Tanaka, 2016 [↗](#)). Therefore, there is theoretically broader scope for experience-dependent reweighting of inputs (Beyeler et al., 2017 [↗](#); Makin & Krakauer, 2023 [↗](#)) and to optimise use of inputs that are still available, more reliable, or more relevant in the impaired system. Conversely, higher-order visual areas may appear more plastic simply because they integrate the cumulative effects of learning from multiple lower stages (Beyeler et al., 2017 [↗](#)).

We propose a hierarchical model of neural adaptation that hypothetically could act to improve the limitations of a rod-only visual system, lacking foveal input and acuity. However, to confirm that the adjustments we observe are truly compensatory rather than mere by-products of circuitry responses to visual deprivation, their functional benefits will need to be demonstrated. The adaptations might suggest that individuals with achromatopsia exhibit superior rod-based vision compared to typical systems. One study supporting this, reported improved rod-mediated biological motion processing in some achromatopsia patients, suggesting an enhanced rod system capacity (Burton et al., 2016 [↗](#)). Nonetheless, most studies typically find achromatopsia patients'

rod vision to be similar or worse, potentially because retinal structure can also be impacted by the disease (Burton et al., 2016 [↗](#); Hess & Nordby, 1986 [↗](#)). It is likely that the functional outcome is shaped by a mixture of impairments and compensatory mechanisms at various levels, which will be important to unpack.

In light of breakthrough treatments set up to restore cone function in human patients with achromatopsia (Farahbakhsh et al., 2022 [↗](#); Fischer et al., 2020 [↗](#); Michaelides et al., 2023 [↗](#); Reichel et al., 2022 [↗](#)), the new plasticity dynamics revealed by our work have significant theoretical and practical implications. The possible dormancy of retinotopic maps in cortical input stages as well as some preserved connectivity between V1 foveal areas and V3 bodes well for these gene therapies, each indicating remaining infrastructure to process rescued cone signals. However, our findings also show that the interpretation of signals from V1 by higher-order networks is modified, and it remains to be seen how this affects the translation of new sensory inputs into functional vision. Adaptations in neuronal tuning properties vary in how stably ingrained they become in neural architecture. They can temporarily shift in response to task-demands (transient modulation) (e.g., Klein et al., 2018 [↗](#)), or unfold over longer periods with extensive experience that can be acquired or reversed at any age (perceptual learning) (Lu & Doshier, 2022 [↗](#)). They can also involve more profound reweighting of neural properties that do not easily revert after critical developmental windows (developmental divergence) (Mitchell & Maurer, 2022). Understanding whether the adaptations in achromatopsia are within the normal range of flexibility for a typically developed system or represent a fundamental reorganisation will be of high relevance to treatment development, as it impacts the nature and extent of neural plasticity that can be harnessed for therapeutic recovery at different ages.

Our findings on hierarchical adaptation have broader implications for other visual disorders, depending on their timing and nature. For instance, a central scotoma acquired in adulthood, as in macular degeneration, may not trigger the same V3 sampling shifts (Haak et al., 2016), suggesting a sensitive window for this form of plasticity, after which connective fields remain more stable. This also raises questions about congenital blindness, where the absence of any driving input could lead to weakening or repurposing of hierarchical connections (Saccone et al., 2024 [↗](#)). Moreover, principles may differ between a deprived but structurally intact cortex, as in retinal dystrophies, and a physically damaged cortex, as in stroke. In the latter, more extensive reorganisation may be required to sample effectively from surviving, and potentially disparate, regions of V1. Perceptual training effects in stroke rehabilitation may reflect such dynamics (Cavanaugh et al., 2025 [↗](#); Elshout et al., 2021 [↗](#)).

With over 50 interventional studies for inherited retinal diseases initiated, the technology to treat these currently incurable diseases by restoring ocular cellular structure and function is here. The next big hurdle will be to understand neural plasticity constraints on integrating new signals from the eye into the existing neural infrastructure. Our research provides a novel framework for understanding the interactions of neural stability and plasticity as the human brain adapts to altered information. The strength of this approach lies in its use of converging evidence from complementary imaging measures and models. Though each has individual limitations, their combination provides robust support for their underlying mechanisms which are of crucial importance for harnessing the full potential of emerging visual restoration therapies.

## Methods

### Participants

All participants met MRI safety inclusion criteria and had no other known neurological disorders. Patients with achromatopsia had genetically confirmed disease (*CNGA3* or *CNGB3* bi-allelic disease-causing variants). The main dataset was collected at 1.5T. Additional structural data was collected at 3T.

## Main 1.5T dataset

We obtained functional and structural 1.5T data from fourteen individuals with achromatopsia (age range = 8-27; mean±std = 13.7±5.7), and forty normally sighted controls (age range=6-34; mean±std=19.8±8.3). Additional structural 1.5T data was collected from 8 achromats (age range=8-35; mean±std=19.75±10.6) and 50 normally sighted controls (age range=6-29; mean±std=12.5±5.9).

## Additional 3T dataset (previously published in Anderson et al. 2024 [↗](#))

We obtained additional structural scans from ten normally sighted controls (age range=20-30; mean±std=23.8±3.7) and 9 individuals with achromatopsia (age range=16-33; mean±std=24.2±6.4).

For 4 normally sighted individuals the rod-only pRF map was not collected. One achromat was excluded from functional analysis due to large head-movements. Data collection had ethics approval from the national ethics committee for individuals with achromatopsia (REC reference: 12/LO/1196, IRAS code: 106506, REC reference 11/LO/1229) and the UCL Research Ethics Committee for normally sighted control participants (4846/001).

## MRI acquisition

### Structural MRI

All 1.5T participants were scanned in a Siemens Avanto 1.5T MRI scanner with a 30-channel coil (a 32-channel coil customised to remove view obstructions). A high-resolution structural scan was acquired using a T1-weighted 3D MPRAGE (1 mm<sup>3</sup> voxel size, Bandwidth = 190 Hz/Px, 176 partitions, partition TR = 2730, TR = 8.4ms, TE = 3.57, effective T1 = 1000 ms, flip angle = 7 degrees).

All 3T participants were scanned in a Siemens 3T TIM-Trio scanner using a 32-channel head coil. A high-resolution structural scan was acquired using a T1-weighted 3D MDEFT, 1mm isotropic voxels, 176 sagittal slices, 256×240 matrix, TE 2.48ms, TR 7.92ms, TI 910ms.

### Functional MRI

Functional T2\*-weighted multiband 2D echo-planar images were collected using a multi-band sequence with 2.3 mm isotropic voxels (TR = 1000 ms, TE = 55 ms, volumes = 348, flip angle = 75°, MB acceleration factor = 4, Bandwidth = 1628 Hz/Px).

## pRF stimuli and apparatus

Stimuli were presented on an MR-compatible LCD display (BOLDscreen 24, Cambridge Research Systems Ltd., UK; 51 x 32 cm; 1920 x 1200 pixels) viewed through a mirror in the scanner at 105 cm distance. Participants were lying supine in the scanner, with fixation stability recorded where possible via a mirror, with an Eyelink 1000 Plus (SR Research, Ottawa, ON) at the back of bore. Built-in gaze calibration was not possible in achromats due to nystagmus so the camera was calibrated in advance on a healthy eye. Before every other run, patients fixated on a 5-point custom calibration which allowed us to calibrate gaze measures post-hoc (Tailor et al., 2021 [↗](#)). Stimuli were presented using MATLAB (R2016b, MathWorks, Natick, MA, USA), via the Psychophysics Toolbox 3 (Kleiner et al., 2007 [↗](#)).

pRF mapping stimuli comprised a simultaneous rotating ring and contracting/expanding wedge embedded within a contrast-reversing checkerboard with 2Hz reversal rate. Per run, the ring expanded/contracted for 6 cycles (48 secs/cycle) with logarithmic eccentricity scaling (van Dijk et al., 2016 [↗](#)). The wedge (20° angle) rotated clockwise/anticlockwise for 8 cycles (36 sec/cycle). 20-second fixation baselines were embedded at the start, at the mid-point, and end of the run (total run duration 348 secs). The stimuli covered a maximum eccentricity of 8.6°, and moved to a new position each 1-second TR. The stimulus was overlaid with a small white central fixation dot (0.2° VA radius) and a black radial grid to encourage stable fixation. To keep participants engaged, they played a rewarded “kitten rescue mission game” in which they pressed a button when detecting a fixation target luminance change.

The rod-selective (stimulating only rods) and non-selective stimuli (stimulating rods and cones equally) differed in both the colour pair (chromatic pair) used to make up the checkerboard and luminance levels. For an in depth description of stimulus generation and validation see [Farahbakhsh et al., 2022](#). In brief, a silent substitution approach was used to obtain a rod-selective colour pair ([Estévez & Spekreijse, 1982](#)). We generated a single chromatic pair that kept L and M cone contrast constant (i.e., invisible to L and M cones), whilst inducing a contrast response in rods. Since it is only possible to simultaneously silence two photoreceptor types with 3 colour channels, the resulting stimulus was not controlled for S-cone contribution. To eradicate the S-cone response, we presented these stimuli at very low light level (max luminance: 0.02 cd/m<sup>2</sup>). The non-selective stimuli chromatic pair increased rod and L and M cone contrasts equivalently. This stimulus was presented at mesopic luminance levels (max 0.5 cd/m<sup>2</sup>).

Prior to the rods only condition, which always appeared before the non-selective condition participants lay in the scanner for a 15-minute dark adaptation. A group of 10 normally sighted control adults had a longer period of dark adaptation (45 minutes) to test any impact on the resultant pRF maps. However, since we did not find any differences between the two groups they were combined and treated as a single control group. We note that excluding these 10 participants did not change any of the reported results.

## Fixation stability

Participants' gaze was tracked throughout all pRF mapping runs. Collecting reliable gaze data from individuals with nystagmus is a challenge because out of the box calibration procedures mostly fail without stable fixation. To account for this, we implemented a post-hoc custom calibration procedure ([Tailor et al., 2021](#)). The eye-tracker was first pre-calibrated on a typically sighted individual. Then, before every other run, we collected gaze data from a 5-point fixation task (at fixation and above, below, left, and right of fixation at 5° eccentricity). This data allowed us to subsequently map the patient's recorded gaze coordinates to their precise locations on the screen. In 10 out of the 14 achromats we acquired reliable enough data to assess fixation stability.

## Calibration data processing

We first removed the first 0.5 seconds for each fixation location to allow for fixation to arrive on the target. We then performed (a) blink removal, (b) filtered out time points with eye movement velocity outliers ( $\pm 2SD$ ), and (c) filtered out any positions  $>3SDs$  to the left or right of the mean fixation location, and  $>1SD$  above or below. We took the median of the remaining gaze measurements as an approximate fixation estimate. The resulting 5 median fixation locations were used to fit an affine transformation that remapped the recorded gaze positions into screen space.

## Quantifying fixation stability

after applying the transformation of the post-hoc calibration, data was filtered for blinks and extreme velocities ( $<2SD$ ). For each functional run, fixation instability was measured as the standard deviation of gaze x-positions across 1-second windows. Measures were then averaged across the two run repeats.

## MRI pre-processing

Data were preprocessed using *fMRIPrep* 21.0.2 ([Esteban, Blair, et al., 2018](#); [Esteban, Markiewicz, et al., 2018](#); *RRID:SCR\_016216*), which is based on *Nipype* 1.6.1 ([K. Gorgolewski et al., 2011](#); [K. J. Gorgolewski et al., 2018](#); *RRID:SCR\_002502*).

## fmriprep structural data pre-processing

The T1-weighted (T1w) image was corrected for intensity non-uniformity (INU) with *N4BiasFieldCorrection* ([Tustison et al., 2010](#)), distributed with ANTs 2.3.3 ([Avants et al., 2008](#); *RRID:SCR\_004757*), and used as T1w-reference throughout the workflow. The T1w-reference was then skull-stripped with a *Nipype* implementation of the *antsBrainExtraction.sh* workflow (from ANTs), using OASIS30ANTs as target template. Brain tissue segmentation of cerebrospinal

fluid (CSF), white-matter (WM) and gray-matter (GM) was performed on the brain-extracted T1w using fast (FSL 6.0.5.1:57b01774, [RRID:SCR\\_002823](#) [↗](#), [Zhang et al., 2001](#) [↗](#)). Brain surfaces were reconstructed using recon-all (FreeSurfer 6.0.1, [RRID:SCR\\_001847](#) [↗](#), [Dale et al., 1999](#) [↗](#)), and the brain mask estimated previously was refined with a custom variation of the method to reconcile ANTs-derived and FreeSurfer-derived segmentations of the cortical gray-matter of Mindboggle ([RRID:SCR\\_002438](#) [↗](#), [A. Klein et al., 2017](#) [↗](#)). Volume-based spatial normalization to one standard space (MNI152NLin2009cAsym) was performed through nonlinear registration with antsRegistration (ANTs 2.3.3), using brain-extracted versions of both T1w reference and the T1w template. The following template was selected for spatial normalization: *ICBM 152 Nonlinear Asymmetrical template version 2009c* [[Fonov et al., 2009](#) [↗](#), [RRID:SCR\\_008796](#) [↗](#); TemplateFlow ID: MNI152NLin2009cAsym]. Many internal operations of fMRIPrep use Nilearn 0.8.1 ([Abraham et al., 2014](#) [↗](#), [RRID:SCR\\_001362](#) [↗](#)), mostly within the functional processing workflow.

### fmrprep functional data pre-processing

For each BOLD run found per subject (across all tasks), the following preprocessing was performed. First, a reference volume and its skull-stripped version were generated by aligning and averaging 1 single-band references (SBRefs). Head-motion parameters with respect to the BOLD reference (transformation matrices, and six corresponding rotation and translation parameters) are estimated before any spatiotemporal filtering using mcflirt (FSL 6.0.5.1:57b01774, [Jenkinson et al., 2002](#) [↗](#)). The BOLD time-series were resampled onto their original, native space by applying the transforms to correct for head-motion. These resampled BOLD time-series will be referred to as *preprocessed BOLD in original space*, or just *preprocessed BOLD*. The BOLD reference was then co-registered to the T1w reference using bbrregister (FreeSurfer) which implements boundary-based registration ([Greve & Fischl, 2009](#) [↗](#)). Co-registration was configured with six degrees of freedom. First, a reference volume and its skull-stripped version were generated using a custom methodology of fMRIPrep. Several confounding time-series were calculated based on the *preprocessed BOLD*: framewise displacement (FD), DVARS and three region-wise global signals. FD was computed using two formulations following Power (absolute sum of relative motions, [Power et al., 2014](#) [↗](#)) and Jenkinson (relative root mean square displacement between affines, [Jenkinson et al., 2002](#) [↗](#)). FD and DVARS are calculated for each functional run, both using their implementations in Nipype (following the definitions by [Power et al., 2014](#) [↗](#)). The three global signals are extracted within the CSF, the WM, and the whole-brain masks.

Additionally, a set of physiological regressors were extracted to allow for component-based noise correction (*CompCor*, [Behzadi et al., 2007](#) [↗](#)). Principal components are estimated after high-pass filtering the *preprocessed BOLD* time-series (using a discrete cosine filter with 128s cut-off) for the two *CompCor* variants: temporal (tCompCor) and anatomical (aCompCor). tCompCor components are then calculated from the top 2% variable voxels within the brain mask. For aCompCor, three probabilistic masks (CSF, WM and combined CSF+WM) are generated in anatomical space. The implementation differs from that of Behzadi et al. in that instead of eroding the masks by 2 pixels on BOLD space, the aCompCor masks are subtracted a mask of pixels that likely contain a volume fraction of GM. This mask is obtained by dilating a GM mask extracted from the FreeSurfer's *aseg* segmentation, and it ensures components are not extracted from voxels containing a minimal fraction of GM. Finally, these masks are resampled into BOLD space and binarized by thresholding at 0.99 (as in the original implementation). Components are also calculated separately within the WM and CSF masks. For each *CompCor* decomposition, the  $k$  components with the largest singular values are retained, such that the retained components' time series are sufficient to explain 50 percent of variance across the nuisance mask (CSF, WM, combined, or temporal). The remaining components are dropped from consideration. The head-motion estimates calculated in the correction step were also placed within the corresponding confounds file. The confound time series derived from head motion estimates and global signals were expanded with the inclusion of temporal derivatives and quadratic terms for each ([Satterthwaite et al. 2013](#)). Frames that exceeded a threshold of 0.9 mm FD or 1.5 standardised DVARS were annotated as motion outliers. The BOLD time-series were resampled onto the following surfaces (FreeSurfer reconstruction nomenclature): *fsnative*. All resamplings can be performed with a *single interpolation step* by

composing all the pertinent transformations (i.e., head-motion transform matrices, susceptibility distortion correction when available, and co-registrations to anatomical and output spaces). Surface resampling was performed using `mri_vol2surf` (FreeSurfer).

### Additional pre-processing

The first 4 volumes of each run were discarded for signal stabilization. Bold data in fsnative space was smoothed along the cortical surface (Gaussian kernel FWHM = 3 mm). For each run, a denoising procedure was further applied on the data by inputting nuisance regressors into a PCA and regressing out the top 5 components. The nuisance regressors include: Six head motion regressors, FD and DVARs, CSF mean signal, white matter mean signal, the first five anatomical CompCor regressors (csf+wm combined), and the first five temporal CompCor regressors. Then data and regressors were temporally filtered with a Savitzky-Golay filter (3rd order, 347 seconds in length) and zscored. The time series from the two identical task runs were then averaged to increase signal to noise ratio.

## MRI analysis

### Region of interests

An anatomically defined retinotopy atlas was applied to the inflated cortical surface for each participant in order to delineate the borders of V1, V2 and V3, and also each degree of eccentricity up to 8° in V1 (Benson & Winawer, 2018 [↗](#)). See Figure 1B [↗](#) for an example of an eccentricity plot for one participant.

### Structural data analysis

The 'mris\_anatomical\_stats' command was used to extract surface area and cortical thickness properties for each participant, per hemisphere, for each region of interest. Overall cortical thickness per participant was computed by weighting the cortical thickness of a hemisphere by the number of vertices per hemisphere.

### pRF analysis

pRF modelling was carried out with a custom Python package, `prfpy` (Aqil & Knapen, 2023 [↗](#)). To model population receptive fields, we used an isometric bivariate Gaussian model (Dumoulin & Wandell, 2008 [↗](#)), with  $x,y$  representing the preferred retinotopic position, spatial standard deviation  $\sigma$  representing pRF size as well as the baseline of the timeseries and the signal amplitude  $\beta$ . At every cortical location, the parameters of each model were optimized by minimizing the residual sum of squares between the model prediction and the measured BOLD signal. Fitting began with a grid search for the best model parameters (pRF position and size) followed by an iterative optimization. In each participant, in each condition, vertices with an  $R^2 < 0.1$  (variance explained by the pRF model), a negative beta, or a centre outside the stimulated radius (8.6°) were excluded from further analysis.

In addition, we ran a second model fit using a stimulus aperture file that incorporated a black oval mask (1.25°x0.96°) over the area of the central rod-free scotoma (Curcio et al., 1990 [↗](#)). Previous research suggests that biases in pRF measures such as shifts in eccentricities and size can occur when a scotoma is present and not explicitly modelled in the stimulus apertures (Binda et al., 2013 [↗](#)). Results from this analysis are reported in Supplement 3.

### Connective field modelling

Connective field modelling was carried out with a dedicated Python package, `prfpy` (Aqil & Knapen, 2023 [↗](#)) based on the method described in Knapen (2021) [↗](#). In brief, gaussian connective field profiles on the surface are defined for each vertex on the cortical manifold, with a centre location of the connective field ( $v$ -centre), and  $\sigma$  (sigma) the Gaussian spread in millimeters on the cortical surface.

To generate spatial Gaussian fields along the V1 surface, the diffusion of heat along the cortical mesh was simulated (Crane et al., 2013 [↗](#)) and used to infer geodesic distances between all V1 vertices (V1 definition was based on the Benson atlas, see Regions of Interest). As the two

hemispheres are two separate surface meshes, this distance matrix was calculated for each hemisphere separately. Grid-fit candidate CF sizes were: [0.5, 1, 2, 3, 4, 5, 7, 10, 15, 20] mm  $\sigma$  for the Gaussian CF. The predicted time course for each of the resulting CF models was generated by taking the dot product between the CF's vertex profile and the vertex by time-courses matrix in V1. The resulting CF model time courses were z scored and correlated with the time courses throughout the brain. For each location in the brain, the connective field resulting in the highest squared correlation was selected. Only values within an  $R^2 > 0.1$ ,  $\beta > 0$ , and a centre within  $8^\circ$  of eccentricity (matching the radius of the stimuli) were included in further analyses. To create connective-field-based eccentricity maps, each vertex was assigned the Benson atlas-based eccentricities (Benson & Winawer, 2018 [DOI](#)) of its CF V1 centre.

For visualisation of group maps all individual maps were transformed to fsaverage space. Plotted values indicate the medians of each group and condition per vertex. A vertex was left empty if no significant data was available for more than 30% of individuals within the group.

## Statistical analysis

Jamovi R package (jmv) was used for Anovas and t-tests (The jamovi project, 2022 [DOI](#)). Jasp (jsq) R package for Bayesian t-tests (JASP team, 2020 [DOI](#)). When sphericity assumptions were not met a greenhouse-geisser correction was applied. Uncorrected p-values are reported as well as FDR multiple comparison corrections.

## Data availability

Because this study involves MRI data from minors with rare conditions, the datasets cannot be made publicly available for confidentiality reasons. Data and code can be requested from the authors.

## Acknowledgements

We thank Maria Molina Sanchez, Hunter Schone and Matan Mazor for providing comments on an earlier version of this manuscript.

## Additional information

### Funding

The research was supported by grants from the National Institute for Health Research (NIHR) Biomedical Research Centre (BRC) at Moorfields Eye Hospital NHS Foundation Trust and UCL Institute of Ophthalmology, the Economic and Social Research Council (ESRC) of the UKRI (#ES/N000838/1); MeiraGTx, Retina UK, Moorfields Eye Charity (R160035A, R190029A, R180004A), Foundation Fighting Blindness (USA) and The Wellcome Trust (099173/Z/12/Z, 100227), Ardalan Family Scholarship, the Persia Educational Foundation Maryam Mirzakhani Scholarship; and the Sir Richard Stapley Educational Trust (#313812). The views expressed are those of the authors and not necessarily those of the NHS, the NIHR, or the Department of Health.

### Funding

Funder	Grant reference number
National Institute for Health Research (NIHR) Biomedical Research Centre (BRC) at Moorfields Eye Hospital NHS Foundation Trust and UCL Institute of Ophthalmology	
Economic and Social Research Council (ESRC) of the UKRI	ES/N000838/1
MeiraGTx	
Retina UK	
Moorfields Eye Charity	R160035A

Moorfields Eye Charity	R190029A
Moorfields Eye Charity	R180004A
Foundation Fighting Blindness	
Wellcome Trust	<a href="https://doi.org/10.35802/099173">https://doi.org/10.35802/099173</a>
Wellcome Trust	<a href="https://doi.org/10.35802/100227">https://doi.org/10.35802/100227</a>

## Author ORCID iDs

**Roni O Maimon-Mor:** <https://orcid.org/0000-0001-5262-9976>

**Tomas Knapen:** <https://orcid.org/0000-0001-5863-8689>

**Tessa M Dekker:** <https://orcid.org/0000-0002-3616-2859>

## Additional files

[Supplementary materials](#) 

## References

- Aboshiha J.,** Dubis A. M., Cowing J., Fahy R. T. A., Sundaram V., Bainbridge J. W., Ali R. R., Dubra A., Nardini M., Webster A. R., *et al.* (2014) A prospective longitudinal study of retinal structure and function in achromatopsia. *Investigative Ophthalmology and Visual Science* **55**:5733-5743  
<https://doi.org/10.1167/iovs.14-14937> | [PubMed](#)
- Abraham A.,** Pedregosa F., Eickenberg M., Gervais P., Mueller A., Kossaifi J., Gramfort A., Thirion B., Varoquaux G (2014) Machine learning for neuroimaging with scikit-learn. *Frontiers in Neuroinformatics* **8** <https://doi.org/10.3389/fninf.2014.00014> | [PubMed](#)
- Adams D. L.,** Sincich L. C., Horton J. C (2007) Complete Pattern of Ocular Dominance Columns in Human Primary Visual Cortex. *Journal of Neuroscience* **27**:10391-10403  
<https://doi.org/10.1523/JNEUROSCI.2923-07.2007> | [PubMed](#)
- Anderson E. J.,** Dekker T. M., Farahbakhsh M., Hirji N., Schwarzkopf D. S., Michaelides M., Rees G (2024) fMRI and gene therapy in adults with CNGB3 mutation. *Brain Research Bulletin* **215**:111026  
<https://doi.org/10.1016/j.brainresbull.2024.111026> | [PubMed](#)
- Aqil M.,** Knapen T (2023) Prfpy: A python package to simulate and fit population receptive field models to time series data. Zenodo. version: v0.1.0-alpha <https://doi.org/10.5281/zenodo.10201022>
- Avants B. B.,** Epstein C. L., Grossman M., Gee J. C (2008) Symmetric diffeomorphic image registration with cross-correlation: Evaluating automated labeling of elderly and neurodegenerative brain. *Medical Image Analysis* **12**:26-41 <https://doi.org/10.1016/j.media.2007.06.004> | [PubMed](#)
- Baker C. I.,** Dilks D. D., Peli E., Kanwisher N (2008) Reorganization of visual processing in macular degeneration: Replication and clues about the role of foveal loss. *Vision Research* **48**:1910-1919  
<https://doi.org/10.1016/j.visres.2008.05.020> | [PubMed](#)
- Baker C. I.,** Peli E., Knouf N., Kanwisher N. G (2005) Reorganization of Visual Processing in Macular Degeneration. *The Journal of Neuroscience* **25**:614-618 <https://doi.org/10.1523/JNEUROSCI.3476-04.2005> | [PubMed](#)
- Barton B.,** Brewer A. A (2015) fMRI of the rod scotoma elucidates cortical rod pathways and implications for lesion measurements. *Proceedings of the National Academy of Sciences of the United States of America* **112**:5201-5206 <https://doi.org/10.1073/pnas.1423673112> | [PubMed](#)
- Baseler H. A.,** Brewer A. A., Sharpe L. T., Morland A. B., Jaägle H., Wandell B. A (2002) Reorganization of human cortical maps caused by inherited photoreceptor abnormalities. *Nature Neuroscience* **5**:364-370 <https://doi.org/10.1038/nn817> | [PubMed](#)
- Baseler H. A.,** Gouws A., Haak K. V., Racey C., Crossland M. D., Tufail A., Rubin G. S., Cornelissen F. W., Morland A. B (2011) Large-scale remapping of visual cortex is absent in adult humans with macular degeneration. *Nature Neuroscience* **14**:649-657 <https://doi.org/10.1038/nn.2793> | [PubMed](#)

- Behzadi Y., Restom K., Liu J., Liu T. T (2007) A component based noise correction method (CompCor) for BOLD and perfusion based fMRI. *NeuroImage* **37**:90-101 <https://doi.org/10.1016/j.neuroimage.2007.04.042> | PubMed
- Benson N. C., Winawer J (2018) Bayesian analysis of retinotopic maps. *eLife* **7** <https://doi.org/10.7554/ELIFE.40224> | PubMed
- Beyeler M., Rokem A., Boynton G. M., Fine I (2017) Learning to see again: Biological constraints on cortical plasticity and the implications for sight restoration technologies. *Journal of Neural Engineering* **14**:051003 <https://doi.org/10.1088/1741-2552/aa795e> | PubMed
- Binda P., Thomas J. M., Boynton G. M., Fine I (2013) Minimizing biases in estimating the reorganization of human visual areas with BOLD retinotopic mapping. *Journal of Vision* **13**:13 <https://doi.org/10.1167/13.7.13> | PubMed
- Brown H. D. H., Gouws A. D., Vernon R. J. W., Lawrence S. J. D., Donnelly G., Gill L., Gale R. P., Baseler H. A., Morland A. B (2021) Assessing functional reorganization in visual cortex with simulated retinal lesions. *Brain Structure and Function* **226**:2855-2867 <https://doi.org/10.1007/s00429-021-02366-w> | PubMed
- Burton E., Wattam-Bell J. S., Rubin G., Aboshiha J., Michaelides M., Atkinson J., Braddick O., Nardini M. (2016) Dissociations in Coherence Sensitivity Reveal Atypical Development of Cortical Visual Processing in Congenital Achromatopsia. *Investigative Ophthalmology & Visual Science* **57**:2251-2259 <https://doi.org/10.1167/iovs.15-18414> | PubMed
- Calford M. B., Chino Y. M., Das A., Eysel U. T., Gilbert C. D., Heinen S. J., Kaas J. H., Ullman S (2005) Rewiring the adult brain. *Nature* **438**:E3-E3 <https://doi.org/10.1038/nature04359> | PubMed
- Carvalho J., Renken R. J., Cornelissen F. W (2019) Studying Cortical Plasticity in Ophthalmic and Neurological Disorders: From Stimulus-Driven to Cortical Circuitry Modeling Approaches. *Neural Plasticity* **2019**:e2724101 <https://doi.org/10.1155/2019/2724101> | PubMed
- Carvalho J., Renken R. J., Cornelissen F. W (2021) Predictive masking of an artificial scotoma is associated with a system-wide reconfiguration of neural populations in the human visual cortex. *NeuroImage* **245**:118690 <https://doi.org/10.1016/j.neuroimage.2021.118690> | PubMed
- Cavanaugh M. R., Fahrenthold B. K., Huxlin K. R (2025) What V1 Damage Can Teach Us About Visual Perception and Learning. *Annual Review of Vision Science* **11**:217-241 <https://doi.org/10.1146/annurev-vision-110323-112823> | PubMed
- Crane K., Weischedel C., Wardetzky M (2013) Geodesics in heat: A new approach to computing distance based on heat flow. *ACM Transactions on Graphics* **32**:152-1 <https://doi.org/10.1145/2516971.2516977>
- Curcio C. A., Sloan K. R., Kalina R. E., Hendrickson A. E (1990) Human photoreceptor topography. *Journal of Comparative Neurology* **292**:497-523 <https://doi.org/10.1002/cne.902920402> | PubMed
- Dale A. M., Fischl B., Sereno M. I (1999) Cortical Surface-Based Analysis: I. Segmentation and Surface Reconstruction. *NeuroImage* **9**:179-194 <https://doi.org/10.1006/nimg.1998.0395> | PubMed
- Dilks D. D., Baker C. I., Peli E., Kanwisher N (2009) Reorganization of Visual Processing in Macular Degeneration Is Not Specific to the "Preferred Retinal Locus". *The Journal of Neuroscience* **29**:2768 <https://doi.org/10.1523/JNEUROSCI.5258-08.2009> | PubMed
- Dumoulin S. O., Knapen T (2018) How Visual Cortical Organization Is Altered by Ophthalmologic and Neurologic Disorders. *Annual Review of Vision Science* **4**:357-379 <https://doi.org/10.1146/annurev-vision-091517-033948> | PubMed
- Dumoulin S. O., Wandell B. A (2008) Population receptive field estimates in human visual cortex. *NeuroImage* **39**:647-660 <https://doi.org/10.1016/j.neuroimage.2007.09.034> | PubMed
- Elshout J. A., Bergsma D. P., van den Berg A. V., Haak K. V. (2021) Functional MRI of visual cortex predicts training-induced recovery in stroke patients with homonymous visual field defects. *NeuroImage: Clinical* **31**:102703 <https://doi.org/10.1016/j.nicl.2021.102703> | PubMed

- Esteban O., Blair R., Markiewicz C. J., Berleant S. L., Moodie C., Ma F., Isik A. I., Erramuzpe A., Kent M., James D., *et al.* (2018) fMRIprep. *Software* <https://doi.org/10.5281/zenodo.852659>
- Esteban O., Markiewicz C., Blair R. W., Moodie C., Isik A. I., Erramuzpe Aliaga A., Kent J., Goncalves M., DuPre E., Snyder M., *et al.* (2018) fMRIprep: A robust preprocessing pipeline for functional MRI. *Nature Methods* <https://doi.org/10.1038/s41592-018-0235-4> | PubMed
- Estévez O., Spekreijse H (1982) The 'silent substitution' method in visual research. *Vision Research* **22**:681-691 [https://doi.org/10.1016/0042-6989\(82\)90104-3](https://doi.org/10.1016/0042-6989(82)90104-3) | PubMed
- Farahbakhsh M., Anderson E. J., Maimon-Mor R. O., Rider A., Greenwood J. A., Hirji N., Zaman S., Jones P. R., Schwarzkopf D. S., Rees G., *et al.* (2022) A demonstration of cone function plasticity after gene therapy in achromatopsia. *Brain* **145**:3803-3815 <https://doi.org/10.1093/brain/awac226> | PubMed
- Ferreira S., Pereira A. C., Quendera B., Reis A., Silva E. D., Castelo-Branco M (2016) Primary visual cortical remapping in patients with inherited peripheral retinal degeneration. *NeuroImage : Clinical* **13**:428-438 <https://doi.org/10.1016/j.nicl.2016.12.013> | PubMed
- Fischer M. D., Michalakis S., Wilhelm B., Zobor D., Muehlfriedel R., Kohl S., Weisschuh N., Ochakovski G. A., Klein R., Schoen C., *et al.* (2020) Safety and Vision Outcomes of Subretinal Gene Therapy Targeting Cone Photoreceptors in Achromatopsia: A Nonrandomized Controlled Trial. *JAMA Ophthalmology* **138**:643-651 <https://doi.org/10.1001/jamaophthalmol.2020.1032> | PubMed
- Fonov V., Evans A., McKinsty R., Almlí C., Collins D (2009) Unbiased nonlinear average age-appropriate brain templates from birth to adulthood. *NeuroImage* **47**:S102 [https://doi.org/10.1016/S1053-8119\(09\)70884-5](https://doi.org/10.1016/S1053-8119(09)70884-5)
- Georgiou M., Fujinami K., Michaelides M (2021) Inherited retinal diseases: Therapeutics, clinical trials and end points—A review. *Clinical & Experimental Ophthalmology* **49**:270-288 <https://doi.org/10.1111/ceo.13917> | PubMed
- Goesaert E., Van Baelen M., Spileers W., Wagemans J., Op de Beeck H. P. (2014) Visual Space and Object Space in the Cerebral Cortex of Retinal Disease Patients. *PLoS ONE* **9**:e88248 <https://doi.org/10.1371/journal.pone.0088248> | PubMed
- Gorgolewski K., Burns C. D., Madison C., Clark D., Halchenko Y. O., Waskom M. L., Ghosh S (2011) Nipype: A flexible, lightweight and extensible neuroimaging data processing framework in Python. *Frontiers in Neuroinformatics* **5**:13 <https://doi.org/10.3389/fninf.2011.00013> | PubMed
- Gorgolewski K. J., Esteban O., Markiewicz C. J., Ziegler E., Ellis D. G., Notter M. P., Jarecka D., Johnson H., Burns C., Manhães-Savio A., *et al.* (2018) Nipype. *Software* <https://doi.org/10.5281/zenodo.596855>
- Greve D. N., Fischl B (2009) Accurate and robust brain image alignment using boundary-based registration. *NeuroImage* **48**:63-72 <https://doi.org/10.1016/j.neuroimage.2009.06.060> | PubMed
- Haak K. V., Cornelissen F. W., Morland A. B (2012) Population Receptive Field Dynamics in Human Visual Cortex. *PLoS ONE* **7**:e37686 <https://doi.org/10.1371/journal.pone.0037686> | PubMed
- Haak K. V., Morland A. B., Engel S. A (2015) Plasticity, and its limits, in adult human primary visual cortex. *Multisensory Research* **28**:297-307 <https://doi.org/10.1163/22134808-00002496> | PubMed
- Haak K. V., Winawer J., Harvey B. M., Renken R., Dumoulin S. O., Wandell B. A., Cornelissen F. W (2013) Connective field modeling. *NeuroImage* **66**:376-384 <https://doi.org/10.1016/j.neuroimage.2012.10.037> | PubMed
- Hess R. F., Nordby K (1986) Spatial and temporal limits of vision in the achromat. *The Journal of Physiology* **371**:365-385 <https://doi.org/10.1113/jphysiol.1986.sp015981> | PubMed
- Hummer A., Ritter M., Woletz M., Ledolter A. A., Tik M., Dumoulin S. O., Holder G. E., Schmidt-Erfurth U., Windischberger C (2018) Artificial scotoma estimation based on population receptive field mapping. *NeuroImage* **169**:342-351 <https://doi.org/10.1016/j.NEUROIMAGE.2017.12.010> | PubMed
- JASP team (2020) Jasp. version: 0.18.3 <https://jasp-stats.org/>
- Jenkinson M., Bannister P., Brady M., Smith S (2002) Improved Optimization for the Robust and Accurate Linear Registration and Motion Correction of Brain Images. *NeuroImage* **17**:825-841 <https://doi.org/10.1006/nimg.2002.1132>

- Jiang J., Zhu W., Shi F., Liu Y., Li J., Qin W., Li K., Yu C., Jiang T (2009) Thick Visual Cortex in the Early Blind. *Journal of Neuroscience* **29**:2205-2211 <https://doi.org/10.1523/JNEUROSCI.5451-08.2009> | PubMed
- Jones P. R., Somoskeöy T., Chow-Wing-Bom H., Crabb D. P (2020) Seeing other perspectives: Evaluating the use of virtual and augmented reality to simulate visual impairments (OpenVisSim). *Npj Digital Medicine* **3**:1-9 <https://doi.org/10.1038/s41746-020-0242-6> | PubMed
- Klein A., Ghosh S. S., Bao F. S., Giard J., Häme Y., Stavsky E., Lee N., Rossa B., Reuter M., Neto E. C., et al. (2017) Mindboggling morphometry of human brains. *PLOS Computational Biology* **13**:e1005350 <https://doi.org/10.1371/journal.pcbi.1005350> | PubMed
- Klein B. P., Fracasso A., van Dijk J. A., Paffen C. L. E., te Pas S. F., Dumoulin S. O. (2018) Cortical depth dependent population receptive field attraction by spatial attention in human V1. *NeuroImage* **176**:301-312 <https://doi.org/10.1016/j.neuroimage.2018.04.055> | PubMed
- Kleiner M., Brainard D. H., Pelli D. G., Broussard C., Wolf T., Niehorster D (2007) What's new in Psychtoolbox-3? A free cross-platform toolkit for psychophysiscs with Matlab and GNU/Octave. *Cognitive and Computational Psychophysics* **36**
- Knapen T (2021) Topographic connectivity reveals task-dependent retinotopic processing throughout the human brain. *Proceedings of the National Academy of Sciences* **118**:e2017032118 <https://doi.org/10.1073/pnas.2017032118> | PubMed
- Kohl S., Jäggle H., Wissinger B., Zobor D. (1993) Achromatopsia. In: Adam M. P., Feldman J., Mirzaa G. M., Pagon R. A., Wallace S. E., Amemiya A. (Eds). *GeneReviews*® University of Washington, Seattle. <http://www.ncbi.nlm.nih.gov/books/NBK1418/> | PubMed
- Lehky S. R., Tanaka K (2016) Neural representation for object recognition in inferotemporal cortex. *Current Opinion in Neurobiology* **37**:23-35 <https://doi.org/10.1016/j.conb.2015.12.001> | PubMed
- Lu Z.-L., Doshier B. A (2022) Current directions in visual perceptual learning. *Nature Reviews Psychology* **1**:654-668 <https://doi.org/10.1038/s44159-022-00107-2> | PubMed
- Macnamara A., Chen C., Schinazi V. R., Saredakis D., Loetscher T (2021) Simulating Macular Degeneration to Investigate Activities of Daily Living: A Systematic Review. *Frontiers in Neuroscience* **15** <https://doi.org/10.3389/fnins.2021.663062> | PubMed
- Makin T. R., Krakauer J. W (2023) Against cortical reorganisation. *eLife* **12**:e84716 <https://doi.org/10.7554/eLife.84716> | PubMed
- Mckyton A., Averbukh E., Marks Ohana D., Levin N., Banin E (2021) Cortical Visual Mapping following Ocular Gene Augmentation Therapy for Achromatopsia. *J Neurosci* **41**:7363-7371 <https://doi.org/10.1523/JNEUROSCI.3222-20.2021> | PubMed
- Michaelides M., Hirji N., Wong S. C., Besirli C. G., Zaman S., Kumaran N., Georgiadis A., Smith A. J., Ripamonti C., Gottlob I., et al. (2023) First-in-Human Gene Therapy Trial of AAV8-hCARp.hCNGB3 in Adults and Children With CNGB3-associated Achromatopsia. *American Journal of Ophthalmology* **253**:243-251 <https://doi.org/10.1016/j.ajo.2023.05.009> | PubMed
- Molz B., Herbik A., Baseler H. A., de Best P. B., Vernon R. W., Raz N., Gouws A. D., Ahmadi K., Lowndes R., McLean R. J., et al. (2022) Structural changes to primary visual cortex in the congenital absence of cone input in achromatopsia. *NeuroImage: Clinical* **33**:102925 <https://doi.org/10.1016/J.NICL.2021.102925> | PubMed
- Molz B., Herbik A., Baseler H. A., de Best P., Raz N., Gouws A., Ahmadi K., Lowndes R., McLean R. J., Gottlob I., et al. (2023) Achromatopsia—Visual Cortex Stability and Plasticity in the Absence of Functional Cones. *Investigative Ophthalmology & Visual Science* **64**:23 <https://doi.org/10.1167/iovs.64.13.23> | PubMed
- Park H.-J., Lee J. D., Kim E. Y., Park B., Oh M.-K., Lee S., Kim J.-J (2009) Morphological alterations in the congenital blind based on the analysis of cortical thickness and surface area. *NeuroImage* **47**:98-106 <https://doi.org/10.1016/j.neuroimage.2009.03.076> | PubMed

- Power J. D., Mitra A., Laumann T. O., Snyder A. Z., Schlaggar B. L., Petersen S. E (2014) Methods to detect, characterize, and remove motion artifact in resting state fMRI. *NeuroImage* **84**:320-341 <https://doi.org/10.1016/j.neuroimage.2013.08.048> | PubMed
- Reichel F. F., Michalakis S., Wilhelm B., Zobor D., Muehlfriedel R., Kohl S., Weisschuh N., Sothilingam V., Kuehlewein L., Kahle N., et al. (2022) Three-year results of phase I retinal gene therapy trial for CNGA3-mutated achromatopsia: Results of a non randomised controlled trial. *British Journal of Ophthalmology* **106**:1567-1572 <https://doi.org/10.1136/bjophthalmol-2021-319067> | PubMed
- Ritter M., Hummer A., Ledolter A. A., Holder G. E., Windischberger C., Schmidt-Erfurth U. M (2019) Correspondence between retinotopic cortical mapping and conventional functional and morphological assessment of retinal disease. *British Journal of Ophthalmology* **103**:208-215 <https://doi.org/10.1136/bjophthalmol-2017-311443> | PubMed
- Saccone E. J., Tian M., Bedny M (2024) Developing cortex is functionally pluripotent: Evidence from blindness. *Developmental Cognitive Neuroscience* **66**:101360 <https://doi.org/10.1016/j.dcn.2024.101360> | PubMed
- Schumacher E. H., Jacko J. A., Primo S. A., Main K. L., Moloney K. P., Kinzel E. N., Ginn J (2008) Reorganization of visual processing is related to eccentric viewing in patients with macular degeneration. *Restorative Neurology and Neuroscience* **26**:391-402 <https://doi.org/10.3233/rnn-2008-00423> | PubMed
- Taylor V. K., Theodorou M., Dahmann-Noor A. H., Dekker T. M., Greenwood J. A (2021) Eye movements elevate crowding in idiopathic infantile nystagmus syndrome. *Journal of Vision* **21**:9-9 <https://doi.org/10.1167/JOV.21.13.9> | PubMed
- Tangtartharakul G., Morgan C. A., Rushton S. K., Schwarzkopf D. S (2023) Retinotopic connectivity maps of human visual cortex with unconstrained eye movements. *Human Brain Mapping* **44**:5221-5237 <https://doi.org/10.1002/hbm.26446> | PubMed
- The jamovi project team (2022) Jamovi. version: 2.3 <https://www.jamovi.org>
- Tustison N. J., Avants B. B., Cook P. A., Zheng Y., Egan A., Yushkevich P. A., Gee J. C (2010) N4ITK: Improved N3 Bias Correction. *IEEE Transactions on Medical Imaging* **29**:1310-1320 <https://doi.org/10.1109/TMI.2010.2046908> | PubMed
- van Dijk J. A., de Haas B., Moutsiana C., Schwarzkopf D. S. (2016) Intersession reliability of population receptive field estimates. *NeuroImage* **143**:293-303 <https://doi.org/10.1016/j.neuroimage.2016.09.013> | PubMed
- Wandell B. A., Smirnakis S. M (2010) Plasticity and stability of visual field maps in adult primary visual cortex. *Nature Reviews Neuroscience* **10**:873-884 <https://doi.org/10.1038/nrn2741> | PubMed
- Zhang Y., Brady M., Smith S (2001) Segmentation of brain MR images through a hidden Markov random field model and the expectation-maximization algorithm. *IEEE Transactions on Medical Imaging* **20**:45-57 <https://doi.org/10.1109/42.906424> | PubMed

## Peer reviews

### Reviewer #1 (Public review):

Summary:

This paper examines plasticity in early cortical (V1-V3) areas in an impressively large number of rod monochromats (individuals with achromatopia). The paper examines three things:

(1) Cortical thickness. It is now well established that early complete blindness leads to increases in cortical thickness. This paper shows increased thickness confined to the foveal projection zone within achromats. This paper replicates work by Molz (2022) and Lowndes

(2021), but the detailed mapping of cortical thickness as a function of eccentricity and the inclusion of higher retinotopic areas is particularly elegant.

(2) Failure to show largescale reorganization of early visual areas using retinotopic mapping. This is a replication of a very recent study of Molz et al. but I believe, given anatomical variability, the larger n in this study, and how susceptible pRF findings are to small changes in procedure, this replication is also of interest.

(3) Connective field modelling, examining the connections between V3-V1. The paper finds changes in the pattern of connections, and smaller connective fields in individuals with achromatopsia than normally sighted controls, and suggests that these reflect compensatory plasticity, with V3 compensating for the lower resolution V1 signal in individuals with achromatopsia.

This is a carefully done study (both in terms of data collection and analysis) that is an impressive amount of work.

#### \*Effects of eye-movements

The authors have carried out the eye-movement analyses I asked of them. Unfortunately, in 4 individuals they couldn't calibrate the eyetracker (it's impressive they managed in 10). I think this means that 4 of 13 (since a different participant was excluded from head motion) individuals weren't included in correlation analyses. Limiting the correlation analysis to individuals with better fixation has obvious issues. I'd recommend redoing (or additionally including) stats using non-parametric measures while classifying these 4 as having fixation instability of 3 (i.e. greater instability than the participant with the worst fixation who was successfully calibrated).

#### \*Interpreting pRFs

The paper would be strengthened by a little more explicit clarity about what pRFs represent and how that affects their interpretation of their findings as plasticity vs. non-plasticity (I know the authors are aware of this, but I think it would be helpful for readers who are less experienced in pRFs). In the introduction it would be helpful to point out that pRFs represent the collective response of a large population of neurons, and as a result pRF estimates can vary depending on which population of neurons that stimulus drives.

For example, imagine for the sake of argument that rods only project to V1 neurons with larger receptive fields. If one measured pRFs in a control observer under photopic vs. scotopic conditions one would see smaller pRFs in the photopic conditions. This wouldn't represent 'plasticity' - it would represent the fact that the firing neurons contributing to the pRF signal are a slightly different population because of a change in the stimulus content. This is of course exactly what you see in 2C. And indeed, the authors make this identical point ". In the non-selective condition, the smaller pRFs in controls are in line with the higher spatial resolution of the

cone system, which is not active in the achromat group." But this point would be clearer if more of the conceptual underpinnings were made explicit in the introduction (or at this point in the paper).

Shifts in which population of neurons drive your pRFs can explain main of the more puzzling results in the paper without detracting from your main conclusions. For example, in 2D, I don't think it's differences in S/N driving your results (pRFs are at least theoretically meant to be robust to S/N). If smaller RFs 'drop out' under low luminance and these smaller RFs also tend to be more central, then one would expect the control results of 1D. And I think a similar argument might even be made for the smaller difference in the rod monochromats.

It would be possible to make the point of Figure 4B more simply if Figure 4B was replaced by additional Panels in Figure 2 simply showing V3 pRF sizes/eccentricity distributions. That would make the point that you don't see the same expansion in pRF sizes in V3 in a way that is just as clear, and is closer to the data.

#### \*Interpreting cRFs

Similarly, I think the paper would be improved with more clarity about the underlying signal in CF modeling. Once again, I appreciate that the authors are familiar with this, but it will help the reader in interpretation. (And I do believe thinking carefully about this may alter your interpretations). CF receptive fields 'find' the region in V1 that best predict the V3 signal in a given voxel. In resting state this likely represents a combination of:

(1) visually driven signal - correlations that may or may not reflect connectivity but represent the fact that regions that represent the same region of visual space will be active at the same time.

(2) global bilaterally symmetrical signal consisting of enhanced correlations between iso-eccentric regions (Raemaekers et al., 2014), which may arise from vasculature that symmetrically stems from the posterior cerebral artery (Tong et al., 2013; Tong and Frederick, 2014).

(3) intrinsic neural fluctuations that are more strongly correlated between connected neurons. These are likely quite weak compared to the other contributions.

I think if you ignore 2, (which is not likely to differ between rod mono and controls) and model 1 and 3, you might well see shifts in CFs towards the boundary of the scotoma - essentially the CF's location will be biased towards the region of V1 that has stronger correlations - which = the region which has a visual signal.

I do find convincing the argument that you don't see the same shift in controls in the rod-selective condition. So I think the results of 4A are fine. But a little more clarity about 'what's under the hood' in CF modeling would be nice.

#### \*Interpreting the relationship between pRFs and cRFs

So there's something here that confuses me. We are all agreed that V3 pRF sizes are similar across RM and control. V1 pRFs are larger in RM. It feels intuitive that smaller CFs would compensate but I can't make it make sense to myself when I think it through. Each pRF represents a combination of receptive field location scatter and bandwidth. You want to argue that eccentricity mapping looks pretty normal, so there's no reason to think increased rf scatter, and I can believe that (though I do think this assumption should be discussed explicitly).

So far I think we agree.

But let's think about what drives a CF during visual stimulation ... Specifically let's think about 'the pRF of the CF' (the region of visual space represented by the cluster of voxels in the CF). If pRFs for individual voxels in V1 are big, then the pRF for the CF is also going to be large. But we know that pRFs for V3 are normal size. So, the V3 CF will 'find' a smaller number of voxels in V1, in order to try to find the 'correct sized' CF pRF. Note that this explanation is very similar to yours. But doesn't require ANY 'intrinsic' connectivity. It's really just assuming the whole thing is driven by the visual signal and the CF size is determined by the ratio of the pRF sizes in V3 vs. V1.

One possible solution would be to regress out the visual stimulus and redo this analysis based on the residuals.

<https://doi.org/10.7554/eLife.100404.2.sa2>

### Reviewer #3 (Public review):

#### Summary:

This study addresses a long-standing question in visual neuroscience concerning how the human visual system balances stability and plasticity when sensory input is altered from early in life. Using achromatopsia as a model of lifelong cone deprivation, the authors examine whether early visual cortex undergoes retinotopic reorganization to compensate for the absence of foveal cone input, or whether canonical retinotopic organization is largely preserved. By combining fMRI-based population receptive field (pRF) mapping with connective field (CF) modelling, the authors characterize changes across multiple hierarchical stages of visual processing.

The main findings indicate that primary visual cortex (V1) shows no systematic remapping of the foveal projection zone, whereas extrastriate cortex, particularly V3, exhibits altered patterns of sampling from V1. The authors interpret these results as evidence for hierarchical adaptation, whereby downstream readout mechanisms adjust to make more efficient use of degraded rod-mediated input while preserving early-stage retinotopic organization.

#### Strengths:

A major strength of this work is the use of silent substitution to generate rod-selective stimuli. This approach enables a principled comparison between achromats and typically sighted controls by isolating rod-driven responses in both groups. In doing so, the study overcomes a key limitation of prior work, where differences in cortical organization could often be confounded by differences in photoreceptor class rather than reflecting neural reorganization per se. The inclusion of a rod-driven baseline in controls provides an important reference for distinguishing long-term adaptation from transient or stimulus-driven effects.

Another notable strength is the integration of CF modelling alongside conventional pRF mapping. While pRF analyses alone suggest enlarged receptive fields in V1, consistent with reduced spatial resolution, the CF analysis offers a more mechanistic account by revealing changes in how V3 samples information from the V1 surface. This multi-level modelling approach moves beyond descriptive accounts of cortical map structure and provides a framework for interpreting how downstream areas may adjust their integration strategies under conditions of altered input.

#### Weaknesses:

Although the study is methodologically strong, the central claims regarding stability and compensatory plasticity require clearer conceptual framing and stronger empirical support. Stability is primarily defined as the absence of large-scale retinotopic remapping in V1, yet the presence of significantly enlarged V1 pRFs indicates substantial tuning-level plasticity at the input stage; distinguishing topographic stability from functional reorganization would therefore strengthen the interpretation. Moreover, the proposed compensatory mechanism raises a signal-processing concern, as reduced downstream sampling (smaller CFs in V3) cannot restore spatial information lost due to coarse upstream representations, and may instead limit integration. The mechanistic link between altered CF properties and normalization of extrastriate pRFs is not directly tested, as group differences are not shown to covary across individuals or visual field locations. Finally, the interpretation of these changes as compensatory implies functional benefit, yet no behavioral or performance measures are provided to establish that the observed reorganization preserves or enhances

visual function, leaving open whether these effects reflect adaptive optimization or passive downstream consequences of altered input.

<https://doi.org/10.7554/eLife.100404.2.sa1>

## Author response:

The following is the authors' response to the original reviews.

### **Public Reviews:**

#### **Reviewer #1 (Public review):**

##### *Summary:*

*This paper examines plasticity in early cortical (V1-V3) areas in an impressively large number of rod monochromats (individuals with achromatopia). The paper examines three things:*

*(1) Cortical thickness. It is now well established that early complete blindness leads to increases in cortical thickness. This paper shows increased thickness confined to the foveal projection zone within achromats. This paper replicates the work by Molz (2022) and Lowndes (2021), but the detailed mapping of cortical thickness as a function of eccentricity and the inclusion of higher visual areas is particularly elegant.*

*(2) Failure to show largescale reorganization of early visual areas using retinotopic mapping. This is a replication of a very recent study by Molz et al. but I believe, given anatomical variability (and the very large n in this study) and how susceptible pRF findings are to small changes in procedure, this replication is also of interest.*

*(3) Connective field modelling, examining the connections between V3-V1. The paper finds changes in the pattern of connections, and smaller connective fields in individuals with achromatopsia than normally sighted controls, and suggests that these reflect compensatory plasticity, with V3 compensating for the lower resolution V1 signal in individuals with achromatopsia.*

##### *Strengths:*

*This is a carefully done study (both in terms of data collection and analysis) that is an impressive amount of work. I have a number of methodological comments but I hope they will be considered as constructive engagement - this work is highly technical with a large number of factors to consider.*

##### *Weaknesses:*

#### *(1) Effects of eye-movements*

*I have some concerns with how the effects of eye-movements are being examined. There are two main reasons the authors give for excluding eye-movements as a factor in their results. Both explanations have limitations.*

*(a) The first is that R2 values are similar across groups in the foveal confluence. This is fine as far as it goes, but R2 values are going to be low in that region. So this shows that eye-movements don't affect coverage (the number of voxels that generate a reliable pRF), but doesn't show that eye-movements aren't impacting their other measures.*

We agree with the reviewer that eye movements could affect pRF measures. We have now also included data for all participants where we were able to obtain eye tracking measures

and directly tested this relationship. Relevant results are copied below.

Recap of results: 1) as expected gaze was less stable in achromats than controls, 2) achromats with more stable gaze did not show more activation in the scotoma projections zone, which we might have observed if fixation instability masks signals in this region 3) Gaze instability was not correlated with pRF size and eccentricity across V1 in achromats. We note that the relationship between nystagmus and visual sampling is complex - patients experience a stable image and may sample only during a specific phase of the eye movement. It is therefore not inherently clear if and how nystagmus affects pRF size.

Relevant Manuscript text incorporating these analyses is copied below.

To quantify eye movement, we used the following methods added to the manuscript:

#### “Fixation stability

Participants' gaze was tracked throughout all pRF mapping runs. Collecting reliable gaze data from individuals with nystagmus is a challenge because out of the box calibration procedures mostly fail without stable fixation. To account for this, we implemented a post-hoc custom calibration procedure (Tailor et al., 2021). The eye-tracker was first precalibrated on a typically sighted individual. Then, before every other run, we collected gaze data from a 5-point fixation task (at fixation and above, below, left, and right of fixation at 5 eccentricity). This data allowed us to subsequently map the patient's recorded gaze coordinates to their precise locations on the screen. In 10 out of the 14 achromats we acquired reliable enough data to assess fixation stability.

Calibration data processing: We first removed the first 0.5 seconds for each fixation location to allow for fixation to arrive on the target. We then performed (a) blink removal, (b) filtered out time points with eye movement velocity outliers ( $\pm 2SD$ ), and (c) filtered out any positions  $>3SDs$  to the left or right of the mean fixation location, and  $>1SD$  above or below. We took the median of the remaining gaze measurements as an approximate fixation estimate. The resulting 5 median fixation locations were used to fit an affine transformation that remapped the recorded gaze positions into screen space.

Quantifying fixation stability: after applying the transformation of the post-hoc calibration, data was filtered for blinks and extreme velocities ( $<2SD$ ). For each functional run, fixation instability was measured as the standard deviation of gaze x-positions across 1second windows. Measures were then averaged across the two run repeats.”

We report the resulting new fixation data results as follows:

#### Results (coverage section):

“Another potential confound in our findings is fixation instability. In pRF mapping, which is usually conducted under photopic (cone-dominant) conditions, unstable fixation can cause a signal drop in the foveal projection zone. As expected due to nystagmus, the achromatopsia group showed higher fixation instability compared to controls (*rodselective*:  $t_{(9,08)}=-3.19$ ,  $p=0.01$ ; *non-selective*:  $t_{sub(9,41)}=-4.88$ ,  $p<0.001$  degrees-of-freedom corrected for unequal-variance; see Supplement Figure S2a). However, several lines of evidence suggest this instability cannot fully account for the lack of “filling in” in achromats. First, within the achromat group, we found no correlation between fixation stability and coverage (*rod-selective*:  $spearman-r_{(8)} = -0.36$ ,  $p=0.31$ ; *non-selective*  $spearman-r_{(8)}=0.07$ ,  $p=0.85$ ); Individuals with more stable, control-like fixation did not show more signal inside the scotoma (see Supplement 2). Second, in adults with achromatopsia, typically with less severe nystagmus (Kohl et al., 1993), two recent studies also found absence of filling in (Anderson et al., 2024; Molz et al., 2023).

So, while we cannot fully exclude nystagmus masking foveal signals in the cortex of some patients, this converging evidence from structural and functional MRI measures across different studies and groups, strongly suggests that the deprived cortex does not substantially ‘fill in’ with peripheral rod inputs in achromatopsia.”

Results (pRF size + eccentricity):

“Larger pRFs indicate that neuronal populations in achromats’ V1 cortex, combine information across larger areas in visual space than in typically sighted controls. This could reflect true neural tuning differences as well as be driven by larger eye movement. However, fixation instability in achromats do not significantly correlate with pRF size in our sample (*rod-selective: spearman-r<sub>(8)</sub> = -0.41, p=0.24; non-selective spearman-r<sub>(8)</sub>=0.37,p=0.29*)

It has been shown that fitting artefacts around scotoma edges, can give rise to similar outward eccentricity shifts (Binda et al., 2013). However, when accounting for fitting artefacts around the foveal scotoma edge by modelling the rod-free zone during pRF fitting, pRF size and eccentricity differences remain unchanged (see Supplement 3). Finally, we found no significant correlations between gaze stability and the eccentricity shift (*rod-selective: spearman-r<sub>(8)</sub> = 0.58, p=0.08; non-selective spearman-r<sub>(8)</sub>=0.09,p=0.8, Supplement 4D*)

Together, these analyses reveal subtle differences in how V1 of achromats responds to rod signals outside the foveal zone, which are consistent with results from other studies (Molz et al. 2023, Anderson et al. 2024). While we found no direct evidence that these are being driven by confounding factors such as eye-movements or fitting artefacts, more work is needed to understand the underlying processes that give rise to these shifts.”

The following text has been added to Supplement 2

“As expected, achromats showed significant higher fixation instability compared to controls (as reported in the main text). We found no significant correlation between fixation instability and either coverage, pRF size, eccentricity in achromats. Results of Spearman R correlations in both rod- and non-selective conditions are reported in the figure. We note that the relationship between nystagmus and visual sampling is complex- patients experience a stable image and may sample only during specific eyemovement phases. It is therefore not fully clear if and how nystagmus should give rise to altered pRFs.”

*(b) The authors don't see a clear relationship between coverage and fixation stability. This seems to rest on a few ad hoc examples. (What happens if one plots mean fixation deviation vs. coverage (and sets the individuals who could not be calibrated as the highest value of calibrated fixation deviation. Does a relationship then emerge?).*

*In any case, I wouldn't expect coverage to be particularly susceptible to eye-movements. If a voxel in the cortex entirely projects to the scotoma then it should be robustly silent. The effects of eye-movements will be to distort the size and eccentricity estimates of voxels that are not entirely silent.*

*There are many places in the paper where eye-movements might be playing an important role.*

*Examples include the larger pRF sizes observed in achromats. Are those related to fixation instability?*

We thank the reviewer for their comment. As detailed in our previous response, we have now extracted fixation instability data from additional patients and have expanded our discussion of its potential effects throughout the manuscript.

*Given that fixation instability is expected to increase pRF size by a fixed amount, that would explain why ratios are close to 1 in V3 (Figure 4).*

We agree with the reviewer's point, that the ratio change on its own is not strong evidence of compensation, this analysis was meant to complement the CF result. The plot in Figure 4 is intended to reconcile the connective field (CF) and pRF results. Its purpose is to illustrate that even though larger pRFs in achromats might seem counterintuitive alongside their smaller V3 CF sizes, the pRF data do not contradict the CF findings but they are in fact consistent with one another. We also agree that there are alternative explanations for the differences in pRF size, such as fixation stability, and we have now added this point to the text.

Results (CF size):

“To understand how this finer cortical sampling in V3 (smaller connective fields) impacts visual processing, we consider its effect on population receptive fields (pRFs). In V1, pRF sizes in achromats were significantly larger than in controls for both stimulus conditions, indicating coarser spatial tuning at the cortical input stage (Figure 4C, left). By selectively sampling from a smaller area of the V1 surface (smaller CFs), V3 can effectively compensate for this coarser input. If so, this process should result in a relative normalisation of pRF size in V3 compared to V1 (Figure 4C, right).

To test this prediction, we plotted the ratio of pRF sizes between achromats and controls, where a value of 1 indicates parity between the groups (Figure 4B). As our compensatory connective field hypothesis predicts, the ratio was closer to 1 in V3 than in V1 across both stimulus conditions, confirming the pRF size difference was significantly reduced at the higher cortical stage. Together this shows converging evidence across the two models (pRF and CF) of hierarchical refinement as a possible compensatory mechanism, where V3's altered connectivity helps to normalize the processing of degraded sensory input from V1.”

Discussion:

“The hierarchical reorganisation observed in V3 is unlikely to be driven by fixation instability. Connective field (CF) estimates are robust to eye movements (Tangtartharakul et al., 2023), because they are anchored to V1 inputs rather than absolute screen position. Considered alone, the pRF results could alternatively be explained by eye movements introducing a fixed size offset that affects smaller V1 pRFs more strongly than those in V3. While we found no evidence for this relationship between pRF size and gaze measures in our patients, we cannot fully rule out the possibility. Nevertheless, the internal consistency between the CF and pRF measures provides a more parsimonious account; that sampling across the hierarchy accounts for coarser tuning at the input stage.”

*(2) Topography*

*The claim of no change in topography is a little confusing given that you do see a change in eccentricity mapping in achromats.*

*Either this result is real, in which case there *\*is\** a change in topography, albeit subtle, or it's an artifact.*

*Perhaps these results need a little bit of additional scrutiny.*

*One reason for concern is that you see different functions relating eccentricity to V1 segments depending on the stimulus. That almost certainly reflects biases in the modelling, not reorganization - the curves of Figure 2D are exactly what Binda et al. predict.*

*Another reason for concern is that I'm very surprised that you see so little effect of including/not including the scotoma - the differences seem more like what I'd expect from simply repeating the same code twice. (The quickest sanity check is just to increase the size of the estimated scotoma to be even bigger?).*

We thank the reviewer for their comment. We have double-checked our scotoma modelling, confirming its correct implementation. The results of the scotoma modelling are not identical to the full one, just similar (see below).

Previous studies on “artificial scotomas” (such as the one reported by Binda et al.) have shown mixed results. While Binda and colleagues found that modelling artificial scotomas normalised pRF shifts, others found no effect (Haak et al. 2012, Prabhakaran et al. 2020). Notably, the rod-free zone in achromatopsia is considerably smaller (~0.5° radius) than most tested artificial scotomas. Moreover, it is unclear whether scotoma modelling is beneficial in clinical populations as artificial scotomas (screen-based masking) are not equivalent to retinal scotomas from inactive photoreceptors. A recent achromatopsia study (Anderson et al. 2024) also found no change in pRF estimates with scotoma modelling.

In our scotoma analyses, we found meaningful differences only in the non-selective condition in controls where cones in the rod-free zone are stimulated - which would be the main expected effect of this modelling exercise (see below). In all other conditions (rod-selective in controls, both conditions in achromats), only rods are stimulated, we found no difference in coverage, eccentricity or pRF size when modelling the scotoma likely because the foveal signal is weak/absent, and did not contribute much to pRF estimates in the unmasked analyses.

This means we cannot account for the eccentricity shift as an edge effect with this scotoma model – but we remain cautious about interpreting it as real. This is because first, as we mention in the paper, in the non-selective condition, which has a higher signal-to-noise ratio, the eccentricity estimates in achromats match those of the control group's rod system. Second, it is still possible that the observed shift is an artefact of modelling that was not accounted for by the approach of scotoma modelling.

Our claim of “no change in topography” specifically referred to the absence of “filling-in” as measured by cortical coverage - the percentage of activated tissue regardless of fitted parameters. However, to avoid confusing given the eccentricity and pRF size results we now rephrased our claim.

Abstract:

“Cortical input stages (V1) exhibited high stability, with input-deprived cortex showing no retinotopic remapping and exhibiting structural hallmarks of deprivation.”

Results (pRF eccentricity):

“It has been shown that fitting artefacts around scotoma edges, can give rise to similar outward eccentricity shifts (Binda et al., 2013). However, when accounting for fitting artefacts around the foveal scotoma edge by modelling the rod-free zone during pRF fitting, pRF size and eccentricity differences remain unchanged (see Supplement 3). Finally, we found no significant correlations between gaze stability and the eccentricity shift (*rod-selective*:  $spearman-r_{(8)} = 0.58, p=0.08$ ; *non-selective*  $spearman-r_{(8)}=0.09, p=0.8$ , Supplement 4D)

Together, these analyses reveal subtle differences in how V1 of achromats responds to rod signals outside the foveal zone, which are consistent with results from other studies (Molz et al. 2023, Anderson et al. 2024). While we found no direct evidence that these are being driven

by confounding factors such as eye movements or fitting artefacts, more work is needed to understand the underlying processes that give rise to these shifts.”

To better illustrate the effect of scotoma modelling text has been added to Supplement 3:

“Studies on artificial scotomas, where part of the visual field is masked, suggest that pRF estimates of eccentricity and size can be biased by fitting scotoma-edge artefacts, and that these can be mitigated by modelling the scotoma in the pRF fitting procedure (e.g., Binda et al. 2013).

We therefore repeated the pRF modelling procedure with the rod-scotoma being modelled as a black oval mask ( $1.25^\circ \times 0.9^\circ$ ) over the stimulus aperture model. As expected, a visible difference between the two models is only apparent in the nonselective condition in controls where the cones in the rod-free zone are being stimulated. In all the other conditions (rod-selective in controls, and both stimulation conditions in achromats) only the rods are stimulated, therefore the masked stimulus still matches the retinal activation, and no major differences can be observed. Performing the same statistical tests applied to the full model in the main text yields equivalent results of equivalent coverage in the rod-selective condition, with equivalent coverage across groups ( $t(47) = 0.78$ ,  $p=0.43$ ,  $BF_{10}=0.31$ ) and controls show a higher coverage in the non-selective stimulation condition compared to achromats (Mann  $U(52)=141$ ,  $p<0.01$ ; unequal variance, reverted to non-parametric).

This consistency in pRF properties when modelling the rod scotoma, is in line with previous results from scotoma modelling; While Binda and colleagues found that this normalised pRF shifts, others found no effect (Haak et al. 2012, Prabhakaran et al. 2020). Notably, the rod-free zone in achromatopsia is considerably smaller ( $\sim 0.5^\circ$  radius) than most tested artificial scotomas, and as artificial scotomas (screen-based masking) are not equivalent to retinal scotomas from inactive photoreceptors, it is unclear how artificial scotoma findings generalise to clinical populations. Our results are in line with a recent achromatopsia study (Anderson et al. 2024) which also found no change in pRF estimates with scotoma modelling.”

*I'd also look at voxels that pass an  $R^2>0.2$  threshold for both the non-selective and selective stimulus. Are the pRF sizes the same for both stimuli? Are the eccentricity estimates? If not, that's another clear warning sign.*

Comparable results were obtained when using higher  $R^2$  thresholds. These results are now included in Supplement 6.

### *(3) Connective field modelling*

*Let's imagine a voxel on the edge of the scotoma. It will tend to have a connective field that borders the scotoma, and will be reduced in size (since it will likely exclude the cortical region of V1 that is solely driven by resting state activity). This predicts your rod monochromat data. The interesting question is why this doesn't happen for controls. One possibility is that there is topdown 'predictive' activity that smooths out the border of the scotoma (there's some hint of that in the data), e.g., Masuda and Wandell.*

*One thing that concerns me is that the smaller connective fields don't make sense intuitively. When there is a visual stimulus, connective fields are predominantly driven by the visual signal. In achromats, there is a large swath of cortex (between 1-2.5 degrees) which shows relatively flat tuning as regards eccentricity. The curves for controls are much steeper, See Figure 2b. This predicts that visually driven connective fields should be larger for achromats. So, what's going on?*

The reviewer raises interesting points about the interpretation of our connective field results. The possibility of differential top-down modulation between controls and achromats is intriguing, however it is not supported by the data, if top-down modulation is activating

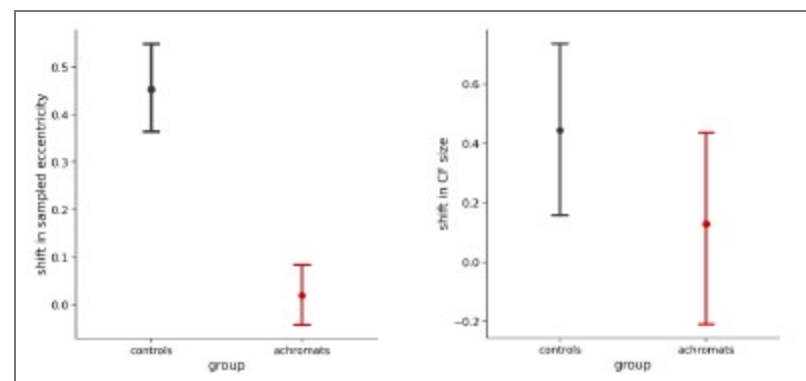
foveal V1 in controls then we shouldn't see a drop in the amount of significant vertices sampling from the fovea in the rod-selective condition compared to the non-selective, but in fact we do see quite a large drop in the amount of significant vertices in that area in the rod-selective condition. Therefore, at the moment we do not think there is strong basis to assume our data could be explained by achromats lacking top-down predictive activity in the scotoma area that is present in controls.

Regarding the concern about smaller CFs seeming counterintuitive given the flat eccentricity tuning in achromats' V1: we believe there is not a straightforward prediction from pRF properties to CF sizes. The relationship between V1 pRF characteristics and V3 CF sampling is complex and not well-established in the literature, and the two can be decoupled to some degree. For instance, in our data, controls show flat V1 pRF sizes in the rod-selective condition (similar to achromats), yet their V3 CF sizes maintain the typical eccentricity-dependent increase seen in the non-selective condition. This suggests that CF size patterns don't simply mirror V1 pRF properties or visual stimuli responses.

Importantly, CF modelling fundamentally differs from pRF analysis in how it might be affected by scotomas. Unlike pRF analysis where a scotoma creates a "silent" region in visual space, in CF modelling the deprived cortex remains physically present and continues generating neural signals (albeit not visually-driven ones). If V3-V1 connectivity were anatomically fixed, V3 would continue sampling from deprived V1 regions even if they do not produce visual-driven signals. A change in this sampling pattern, as we see in our data, is therefore evidence for plasticity.

Our data support this interpretation. First, in achromats, the CF size pattern observed cannot be easily explained by scotoma-edge artefacts. V3 vertices sampling from the immediate vicinity of the scotoma ( $1^{\circ}$ - $3^{\circ}$ ) show CF sizes comparable to controls. The effect is only significant further away from the scotoma ( $4^{\circ}$ - $6^{\circ}$ ).

Second, to assess how the presence of a scotoma affects CF measure we can compare the two conditions in the controls, since the rod-selective condition has a scotoma present and the nonselective condition does not. For this purpose, we performed an additional analysis, quantifying on a vertex-by-vertex level the differences in CF fitted parameters between the two stimulation conditions across V1. See results below. In achromats there are no systematic shifts between the stimulation conditions, as expected as both are rod-driven. In controls, this analysis reveals only subtle shifts ( $\sim 0.45^{\circ}$  in the rod-selective condition). CF size has also changed slightly although not significantly different from that observed in achromats. These shifts are much smaller than the CF size and eccentricity differences between controls and achromats, so we consider it unlikely that our findings are driven by scotoma artefacts.



Author response image 1.

## Results (CF size):

“The significant CF size differences are unlikely to be a model-fitting bias around a scotoma edge, as V3 vertices sampling from the immediate vicinity of the scotoma ( $1^{\circ}3'$ ) show CF sizes comparable to controls. The significant reduction in CF size occurs only further in the periphery ( $4^{\circ}$ - $6^{\circ}$ ), in regions that are primarily stimulus-driven.

To understand how this finer cortical sampling in V3 (smaller connective fields) impacts visual processing, we consider its effect on population receptive fields (pRFs). In V1, pRF sizes in achromats were significantly larger than in controls for both stimulus conditions, indicating coarser spatial tuning at the cortical input stage (Figure 4C, left). By selectively sampling from a smaller area of the V1 surface (smaller CFs), V3 can effectively compensate for this coarser input. If so, this process should result in a relative normalisation of pRF size in V3 compared to V1 (Figure 4C, right).

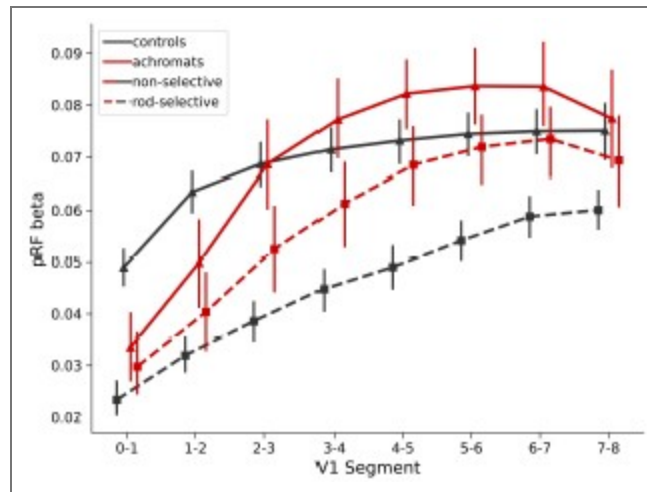
To test this prediction, we plotted the ratio of pRF sizes between achromats and controls, where a value of 1 indicates parity between the groups (Figure 4B). As our compensatory connective field hypothesis predicts, the ratio was closer to 1 in V3 than in V1 across both stimulus conditions, confirming the pRF size difference was significantly reduced at the higher cortical stage. Together this shows converging evidence across the two models (pRF and CF) of hierarchical refinement as a possible compensatory mechanism, where V3's altered connectivity helps to normalize the processing of degraded sensory input from V1.”

## Discussion (added paragraph):

“The hierarchical reorganisation observed in V3 is unlikely to be driven by fixation instability. Connective field (CF) estimates are robust to eye movements (Tangtartharakul et al., 2023), because they are anchored to V1 inputs rather than absolute screen position. Considered alone, the pRF results could alternatively be explained by eye movements introducing a fixed size offset that affects smaller V1 pRFs more strongly than those in V3. While we found no evidence for this relationship between pRF size and gaze measures in our patients, we cannot fully rule out the possibility. Nevertheless, the internal consistency between the CF and pRF measures provides a more parsimonious account; that sampling across the hierarchy accounts for coarser tuning at the input stage.”

| *The beta parameter is not described (and I believe it can alter connective field sizes).*

In Author response image 2, we plot the beta parameter of the pRF modelling in V1 with no  $R^2$  filtering, error bars are 95% CIs:

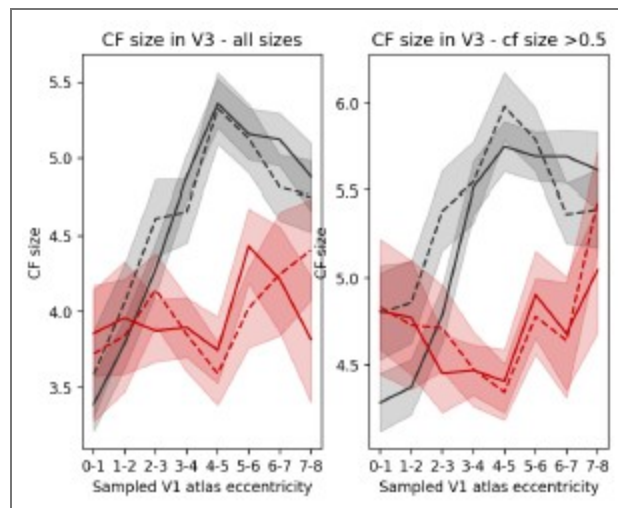


Author response image 2.

The reviewer did not specify how beta might alter connective field sizes. We assume he meant that as in pRF mapping, the slope of activity from deprived to non-deprived cortex will artefactually create a CF model fit with smaller CF sizes. To test this, we calculated the slope of beta values between 0° and 3° in each participant in the rod-selective condition, as this range includes the scotoma and the area at the edge of the scotoma. We then used the slope as a covariate in an ANCOVA when comparing the CF sizes across groups in each sampled V1 segment. Accounting for the beta slope of V1 did not change the reported results. This analysis still shows smaller CF sizes in V3 in the rod-selective conditions between 4°-6° eccentricity – these differences remain significant ( $p < 0.001$  for 4°-5° and  $p < 0.05$  for 5°-6° when comparing achromats vs controls).

*Similarly, it's possible to get very small connective fields, but there wasn't a minimum size described in the thresholding.*

CF sizes were fit with a grid fit. Possible values were [0.5,1,2,3,4,5,7,10]. Therefore, the minimum size is 0.5. Filtering out the smallest connective field sizes does not change the results:



Author response image 3.

*I might be missing something obvious, but I'm just deeply confused as to how the visual maps and the connectome maps can provide contradictory results given that the connectome maps are predominantly determined by the visual signal. Some intuition would be helpful.*

We agree that this appears counterintuitive, and now added further clarification. The two models (pRF and CF) fundamentally differ in what they measure and how they relate to visual processing. V1 pRF sizes reflect the relationship between neural activity and visual stimuli - essentially how much of a visual stimulus drives a voxel's response - while V3 CF sizes reflect how V3 samples from the V1 cortical surface, indicating how many V1 voxels contribute to a V3 voxel's activity.

The measures constrain each other, as a V3 voxel's pRF size is expected to match the pooling of its connected V1 inputs. But they can be decoupled: A V3 voxel could sample from a small area of V1 cortex (a small CF in mm) that happens to represent a large area of visual space if those V1 voxels have large pRFs. The aim of Figure 4B is to clarify that the measures are consistent with one another even though they diverge in direction. In achromats, where V1 voxels have larger pRFs (coarser spatial resolution), V3 appears to compensate by sampling more selectively from V1 via smaller CF sizes. Theoretically, this should reduce the pRF size difference between controls and patients in V3, a prediction that our data supports.

Results (CF size):

“To understand how this finer cortical sampling in V3 (smaller connective fields) impacts visual processing, we consider its effect on population receptive fields (pRFs). In V1, pRF sizes in achromats were significantly larger than in controls for both stimulus conditions, indicating coarser spatial tuning at the cortical input stage (Figure 4C, left). By selectively sampling from a smaller area of the V1 surface (smaller CFs), V3 can effectively compensate for this coarser input. If so, this process should result in a relative normalisation of pRF size in V3 compared to V1 (Figure 4C, right).

To test this prediction, we plotted the ratio of pRF sizes between achromats and controls, where a value of 1 indicates parity between the groups (Figure 4B). As our compensatory connective field hypothesis predicts, the ratio was closer to 1 in V3 than in V1 across both stimulus conditions, confirming the pRF size difference was significantly reduced at the higher cortical stage. Together this shows converging evidence across the two models (pRF and CF) of hierarchical refinement as a possible compensatory mechanism, where V3's altered connectivity helps to normalize the processing of degraded sensory input from V1.”

Discussion (added paragraph):

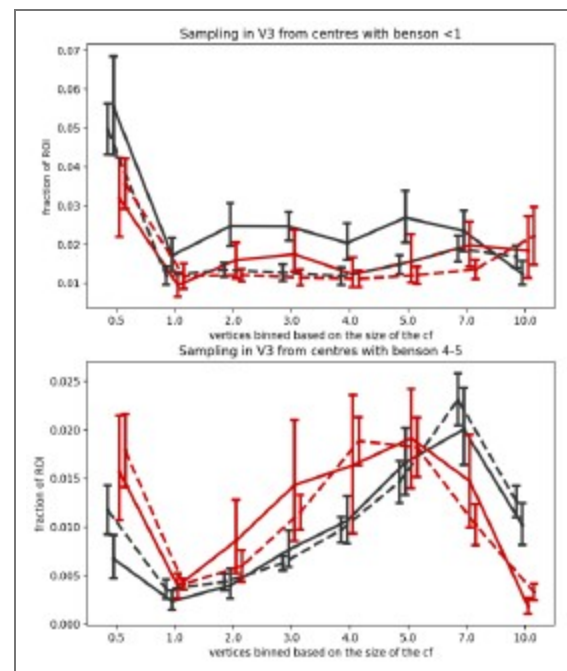
“The hierarchical reorganisation observed in V3 is unlikely to be driven by fixation instability. Connective field (CF) estimates are robust to eye movements (Tangtartharakul et al., 2023), because they are anchored to V1 inputs rather than absolute screen position. Considered alone, the pRF results could alternatively be explained by eye movements introducing a fixed size offset that affects smaller V1 pRFs more strongly than those in V3. While we found no evidence for this relationship between pRF size and gaze measures in our patients, we cannot fully rule out the possibility. Nevertheless, the internal consistency between the CF and pRF measures provides a more parsimonious account; that sampling across the hierarchy accounts for coarser tuning at the input stage.”

*Some analyses might also help provide the reader with insight. For example, doing analyses separately on V3 voxels that project entirely to scotoma regions, project entirely to stimulusdriven regions, and V3 voxels that project to 'mixed' regions.*

We agree that it is important to plot the connective field dynamics across the scotoma region.

In Figure 4A we split the V3 vertices based on the V1 area they sample from. Therefore the  $0^{\circ}$ - $1^{\circ}$  would be considered as mainly sampling from the “scotoma” region and the higher the eccentricity is, the less “scotoma” it includes. The V3 vertices that have a significantly smaller CF size compared to controls are those sampling from mostly if not entirely stimulus-driven regions  $4^{\circ}$ - $5^{\circ}$  and  $5^{\circ}$ - $6^{\circ}$ . We are not sure how further binning the data by within, across and outside scotoma would be more informative.

However, in Author response image 4, we plot in more details the distribution of CF sizes sampling from a V1 segment clearly inside and clearly outside the scotoma. The top figure shows the CF size distribution of V3 vertices that sample from a V1  $0^{\circ}$ - $1^{\circ}$  segment, where V1 is deprived of input due to the rod scotoma. In achromats, there is a clear drop in vertices with a very small (0.5) CF size. The bottom figure shows the distribution of V3 vertices that sample from the V1  $4^{\circ}$ - $5^{\circ}$  segment which falls outside the scotoma and shows a significant difference in CF size across the groups. Here in achromats you can see a drop in larger V3 CF sizes sampling from the V1 region, and an increase in smaller ones (note that this further addresses a previous concern that connective field differences across groups are solely driven by very small CFs).



Author response image 4.

Following the reviewer’s comment we have added the following statement in the results section discussing CF size:

“The significant CF size differences are unlikely to be a model-fitting bias around a scotoma edge, as V3 vertices sampling from the immediate vicinity of the scotoma ( $1^{\circ}$ - $3^{\circ}$ ) show CF sizes comparable to controls. The significant reduction in CF size occurs only further in the periphery ( $4^{\circ}$ - $6^{\circ}$ ), in regions that are primarily stimulus-driven.”

*The finding that pRF sizes are larger in achromats by a constant factor as a function of eccentricity is what differences in eye-movements would predict. It would be worth examining the relationship between pRF sizes and fixation stability.*

We found no relationship between fixation stability and pRF size in V1, although as we explain in response to an earlier point, this does not fully exclude the reviewers alternative explanation, which we now add to the discussion.

Discussion:

“The hierarchical reorganisation observed in V3 is unlikely to be driven by fixation instability. Connective field (CF) estimates are robust to eye movements (Tangtartharakul et al., 2023), because they are anchored to V1 inputs rather than absolute screen position. Considered alone, the pRF results could alternatively be explained by eye movements introducing a fixed size offset that affects smaller V1 pRFs more strongly than those in V3. While we found no evidence for this relationship between pRF size and gaze measures in our patients, we cannot fully rule out the possibility. Nevertheless, the internal consistency between the CF and pRF measures provides a more parsimonious account; that sampling across the hierarchy accounts for coarser tuning at the input stage.”

**Reviewer #2 (Public review):**

*Summary:*

*The authors inspect the stability and compensatory plasticity in the retinotopic mapping in patients with congenital achromatopsia. They report an increased cortical thickness in central (eccentricities 0-2 deg) in V1 and the expansion of this effect to V2 (trend) and V3 in a cohort with an average age of adolescents.*

*In analyzing the receptive fields, they show that V1 had increased receptive field sizes in achromats, but there were no clear signs of reorganization filling in the rod-free area. In contrast, V3 showed an altered readout of V1 receptive fields. V3 of achromats oversampled the receptive fields bordering the rod-free zone, presumably to compensate and arrive at similar receptive fields as in the controls.*

*These findings support a retention of peripheral-V1 connectivity, but a reorganization of later hierarchical stages of the visual system to compensate for the loss, highlighting a balance between stability and compensation in different stages of the visual hierarchy.*

*Strengths:*

*The experiment is carefully analyzed, and the data convey a clear and interesting message about the capacities of plasticity.*

*Weaknesses:*

*The existence of unstable fixation and nystagmus in the patient group is alluded to, but not quantified or modeled out in the analyses. The authors may want to address this possible confound with a quantitative approach.*

We have responded to this in the “Recommendations for the authors” section of this reviewer, as they included a more detailed description of these points there.

**Recommendations for the authors:**

**Reviewer #1 (Recommendations for the authors):**

*(1) I think the term rod monochromats should be included early in the paper since it's a more intuitive term to describe this population.*

We agree with the reviewer that the term “rod monochromats” is more intuitive as it clarifies the retinal source of the disease but have chosen the term achromats for consistency with a

wide literature of published work in this group, including our own and our close collaborators'. To clarify, in the first mention of the group as achromats in the introduction we have now added this term:

“Achromatopsia (also known as rod monochromacy) causes cone photoreceptors in the retina to be inactive from birth (Aboshiha et al., 2014).”

*(2) The paper essentially contains two definitions of 'eccentricity'. One (atlas/segments) comes from the Benson atlas and the other (functional) comes from pRF mapping. It would be good to make this distinction terminology clearer earlier in the paper. It would also be good to use more consistent terminology. I assume 'sampled atlas V1 eccentricity' in 3A is the same as 'V1 segment' in 1A?*

For consistency we have now referred to these as V1 segment and sampled V1 segment in the figures when describing the atlas-based definition, and eccentricity for the measured pRF-based eccentricity.

*(3) The 'stability vs. plasticity' framing in the introduction could be tightened slightly.*

We have made the following changes following the reviewer's comment:

“In the visual domain, the focal point of the debate on plasticity and stability has hinged on the extent to which retinal input deprivation can drive local reorganisation in early visual cortex, for example, for deprived tissue to take on inputs from spared retinal locations (Adams et al., 2007; Baker et al., 2005, 2008; Baseler et al., 2002, 2011; Calford et al., 2005; Dilks et al., 2009; Dumoulin & Knapen, 2018; Ferreira et al., 2016; Goesaert et al., 2014; Haak et al., 2015; Molz et al., 2023; Ritter et al., 2019; Schumacher et al., 2008). In reality visual impairment is a more global phenomenon, affecting all levels of visual processing, with complex dynamics beyond constricted local retinocortical projection zones (Carvalho et al., 2019).”

*(4) Figure 1A, define the x axis as degrees.*

We have now added the ° sign to all the tick labels indicating Benson map eccentricity.

*(5) Figure 2B, is there room for pictures of the silent substitution/standard stimulus*

We have now added images in a Supplement 5 to avoid cluttering the main Figure 2B

*(6) Figure 2*

*Panel A has a slightly weird organization. The reader is supposed to compare the square symbols to each other, and the circles to each other, why not organize the figure so they are adjacent in the graph (i.e. non selective control, non-selective achromat, selective control, selective achromat)? That also helps the reader orient that in the non-selective conditions you have almost complete pRF coverage.*

We have taken on the reviewer's suggestion and changed the order.

*In the inset, maybe use empty symbols? That's the traditional way to say that the square/circle applies to both red and black.*

We prefer the current format.

*Figure 2C - the symbols change to circles? Why not keep the symbols of A?*

We have now changed the symbols of 2C&D.

*I'd put the non-selective maps above the selective maps?*

We appreciate the feedback but prefer to keep it as it is, as we feel the critical point is conveyed by the rod maps.

(7) *'We propose a new hierarchical model of neural adaptation'. These ideas are hardly new. There are also other models, that would explain your data (cumulative plasticity)*  
<https://www.ncbi.nlm.nih.gov/pmc/articles/PMC5953572/>

We thank the reviewer for the reference. We have now cited it in our discussion and removed the word “new” from the mentioned sentence.

“Therefore, there is theoretically broader scope for experience-dependent reweighting of inputs (Beyeler et al., 2017; Makin & Krakauer, 2023) and to optimise use of inputs that are still available, more reliable, or more relevant in the impaired system. Conversely, higher-order visual areas may appear more plastic simply because they integrate the cumulative effects of learning from multiple lower stages (Beyeler et al., 2017).”

We propose a hierarchical model of neural adaptation...” [deleted the word new]

(8) *Line 508. No image of the stimulus is contained in the paper*

Corrected

(9) *Line 620. I believe the Figure is 1B, not 1C.*

Corrected

(10) *Figure 4A. CF Size - add mm<sup>2</sup> to the axes.*

Corrected

**Reviewer #2 (Recommendations for the authors):**

*I am not an expert on pRF mapping, and as such, I am unsure how to relate to pRF mapping performed in patients with unstable fixation (not quantified, but referred to) and nystagmus, such as the achromatic population here. Since the majority of the results hinge on this analysis, I would appreciate more data about the differences between the groups. Supplement 2, which is meant to speak to this, shows only the data from 3 typical participants, and in itself is not evidence for "no correlation between stable fixation and enhanced foveal". Additionally, I'd appreciate a clear methods explanation of how the authors address these confounds; this is too important a concern to be left for the discussion section.*

We agree with the reviewer that eye movements could affect pRF measures. We have now also included data for all participants where we were able to obtain eye tracking measures and directly tested this relationship. Relevant results are copied below.

Recap of results: 1) as expected gaze was less stable in achromats than controls, 2) achromats with more stable gaze did not show more activation in the scotoma projections zone, which we might have observed if fixation instability masks signals in this region 3) Gaze instability was not correlated with pRF size and eccentricity across V1 in achromats. We note that the relationship between nystagmus and visual sampling is complex - patients experience a stable image and may sample only during a specific phase of the eye movement. It is therefore not inherently clear if and how nystagmus affects pRF size.

Relevant Manuscript text incorporating these analyses is copied below.

To quantify eye movement, we used the following methods added to the manuscript:

### “Fixation stability

Participants' gaze was tracked throughout all pRF mapping runs. Collecting reliable gaze data from individuals with nystagmus is a challenge because out of the box calibration procedures mostly fail without stable fixation. To account for this, we implemented a post-hoc custom calibration procedure (Tailor et al., 2021). The eye-tracker was first precalibrated on a typically sighted individual. Then, before every other run, we collected gaze data from a 5-point fixation task (at fixation and above, below, left, and right of fixation at 5 eccentricity). This data allowed us to subsequently map the patient's recorded gaze coordinates to their precise locations on the screen. In 10 out of the 14 achromats we acquired reliable enough data to assess fixation stability.

**Calibration data processing:** We first removed the first 0.5 seconds for each fixation location to allow for fixation to arrive on the target. We then performed (a) blink removal, (b) filtered out time points with eye movement velocity outliers ( $\pm 2SD$ ), and (c) filtered out any positions  $>3SDs$  to the left or right of the mean fixation location, and  $>1SD$  above or below. We took the median of the remaining gaze measurements as an approximate fixation estimate. The resulting 5 median fixation locations were used to fit an affine transformation that remapped the recorded gaze positions into screen space.

**Quantifying fixation stability:** after applying the transformation of the post-hoc calibration, data was filtered for blinks and extreme velocities ( $<2SD$ ). For each functional run, fixation instability was measured as the standard deviation of gaze x-positions across 1second windows. Measures were then averaged across the two run repeats.”

### Results (coverage section):

“Another potential confound in our findings is fixation instability. In pRF mapping, which is usually conducted under photopic (cone-dominant) conditions, unstable fixation can cause a signal drop in the foveal projection zone. As expected due to nystagmus, the achromatopsia group showed higher fixation instability compared to controls (*rodselective*:  $t_{(9,08)}=-3.19$ ,  $p=0.01$ ; *non-selective*:  $t_{(9,41)}=-4.88$ ,  $p<0.001$  degrees-of-freedom corrected for unequal-variance; see Supplement Figure S2a). However, several lines of evidence suggest this instability cannot fully account for the lack of “filling in” in achromats. First, within the achromat group, we found no correlation between fixation stability and coverage (*rod-selective*:  $spearman-r_{(8)} = -0.36$ ,  $p=0.31$ ; *non-selective*  $spearman-r_{(8)}=0.07$ ,  $p=0.85$ ); Individuals with more stable, control-like fixation did not show more signal inside the scotoma (see Supplement 2). Second, in adults with achromatopsia, typically with less severe nystagmus (Kohl et al., 1993), two recent studies also found absence of filling in (Anderson et al., 2024; Molz et al., 2023).

So, while we cannot fully exclude nystagmus masking foveal signals in the cortex of some patients, this converging evidence from structural and functional MRI measures across different studies and groups, strongly suggests that the deprived cortex does not substantially ‘fill in’ with peripheral rod inputs in achromatopsia.”

### Results (pRF size + eccentricity):

“Larger pRFs indicate that neuronal populations in achromats' V1 cortex, combine information across larger areas in visual space than in typically sighted controls. This could reflect true neural tuning differences as well as be driven by larger eye movement. However, fixation instability in achromats do not significantly correlate with pRF size in our sample (*rod-selective*:  $spearman-r_{(8)} = -0.41$ ,  $p=0.24$ ; *non-selective*  $spearman-r_{(8)}=0.37$ ,  $p=0.29$ )

It has been shown that fitting artefacts around scotoma edges, can give rise to similar outward eccentricity shifts (Binda et al., 2013). However, when accounting for fitting artefacts

around the foveal scotoma edge by modelling the rod-free zone during pRF fitting, pRF size and eccentricity differences remain unchanged (see Supplement 3). Finally, we found no significant correlations between gaze stability and the eccentricity shift (*rod-selective*:  $spearman-r_{(8)} = 0.58, p=0.08$ ; *non-selective*  $spearman-r_{(8)}=0.09, p=0.8$ , Supplement 4D)

Together, these analyses reveal subtle differences in how V1 of achromats responds to rod signals outside the foveal zone, which are consistent with results from other studies (Molz et al. 2023, Anderson et al. 2024). While we found no direct evidence that these are being driven by confounding factors such as eye-movements or fitting artefacts, more work is needed to understand the underlying processes that give rise to these shifts.”

The following text has been added to Supplement 2

“As expected, achromats showed significant higher fixation instability compared to controls (as reported in the main text). We found no significant correlation between fixation instability and either coverage, pRF size, eccentricity in achromats. Results of Spearman R correlations in both rod- and non-selective conditions are reported in the figure. We note that the relationship between nystagmus and visual sampling is complex- patients experience a stable image and may sample only during specific eyemovement phases. It is therefore not fully clear if and how nystagmus should give rise to altered pRFs.”

*The field connectivity analysis similarly seems to be used only on task data from the same design; if it was replicated from resting-state data, that would be a good way to show consistency which is independent of measures requiring fixation.*

We agree that resting-state data would be valuable; however, we did not collect such data in these individuals due to time limitations. Instead, we demonstrate the consistency and reliability of our results by replicating our findings across two different stimulation conditions (rod-selective and non-selective), which differ in luminance, contrast and signal amplitude in both groups and for controls also in the photoreceptors involved. The convergence of results across these distinct visual conditions strengthens our confidence in the reliability of the observed effects. Also, notably, CF estimates have been shown to be robust to large eye movements, and therefore also to differences in fixation stability across groups (Tangtartharakul et al., 2023).

*The authors may want to contextualize their findings in relation to what reorganization exists in cases of late-onset loss of part of the visual field on one hand (stroke recovery), and in the case of complete blindness from early life on the other, as both speak to different levels of plasticity the visual system is capable of.*

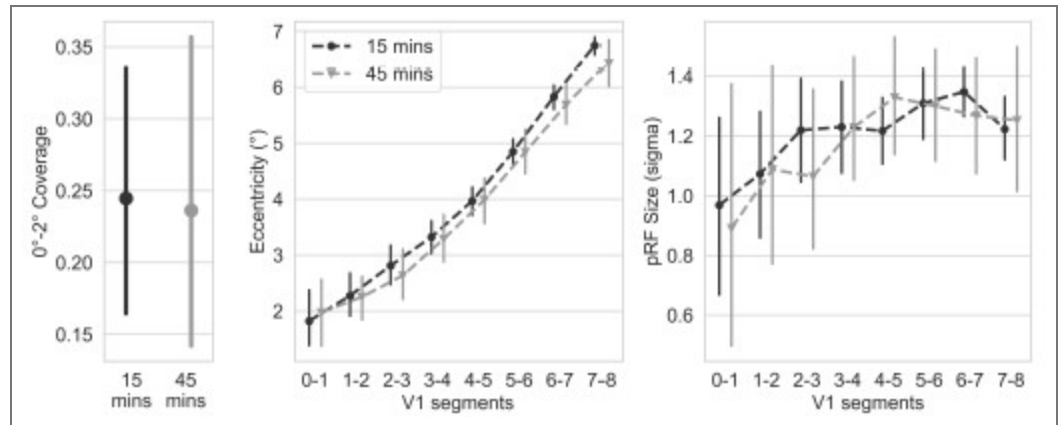
We thank the reviewer for their comment and have added a new paragraph discussing this topic.

Discussion:

“Our findings on hierarchical adaptation have broader implications for other visual disorders, depending on their timing and nature. For instance, a central scotoma acquired in adulthood, as in macular degeneration, may not trigger the same V3 sampling shifts (Haak et al., 2016), suggesting a sensitive window for this form of plasticity, after which connective fields remain more stable. This also raises questions about congenital blindness, where the absence of any driving input could lead to weakening or repurposing of hierarchical connections (Saccone et al., 2024). Moreover, principles may differ between a deprived but structurally intact cortex, as in retinal dystrophies, and a physically damaged cortex, as in stroke. In the latter, more extensive reorganisation may be required to sample effectively from surviving, and potentially disparate, regions of V1. Perceptual training effects in stroke rehabilitation may reflect such dynamics (Cavanaugh et al., 2025; Elshout et al., 2021).”

*A more minor point: Can the authors clarify what the dark adaptation is used for, and provide the supplementary analysis showing that the duration difference for some of the participants didn't impact the results (stated but not shown).*

The dark adaptation period before the rod-selective condition allowed rod photoreceptors to recover from bleaching caused by prior mesopic light exposure, ensuring optimal rod sensitivity under scotopic conditions. To verify that our 15-minute adaptation period was sufficient, we tested 10 control participants with an extended 45-minute adaptation period. As we found no differences in the resulting rod maps between standard and extended adaptation protocols, these participants were combined with the main control group for all analyses. Author response image 5 are the plots for the two dark adaptation periods.



Author response image 5.

<https://doi.org/10.7554/eLife.100404.2.sa0>